Deanship of Graduate Studies
Al – Quds University

Analytical Model Study of Complexation of Linear Polyelectrolyte with a Charged Dendrimer of Different Generations

Azzam Ali Abu khalil

M.Sc. Thesis

Jerusalem – Palestine

1432 / 2011

Deanship of Graduate Studies
Al – Quds University

Analytical Model Study of Complexation of Linear Polyelectrolyte with a Charged Dendrimer of Different Generations

Prepared by:

Azzam Ali Abu khalil

Supervisor: Dr. Khawla Qamhieh

A thesis submitted in partial fulfillment of requirement for the degree of Master of Science in Physics

Jerusalem – Palestine

1432/2011

Deanship of Graduate Studies
Al – Quds University

Thesis Approval

Analytical Model Study of Complexation of Linear Polyelectrolyte with a Charged Dendrimer of Different Generations

Prepared by: Azzam Ali Abu khalil
Registration No: 20812167

Supervisor: Dr. Khawla Qamhieh

Master thesis submitted and accepted, date 29 /12 / 2011

The name and signature of examining committee member are as follows:

1- Head of the committee: Dr. Khawla Qamhieh Signature: .....
2. Internal Examiner: Dr. Mohammad M. Abu-Samreh Signature: .....
3. External Examiner: Dr. Mohammad Abu-Ja´far Signature: .....

Jerusalem – Palestine

1432/2011

Dedication

I dedicate this thesis to my family, especially, to my father and mother for their patience and understanding---- to my brother for opening my eyes to the world.

Declaration

I hereby declare that this thesis is based on the results found by myself. Materials of works found by other researchers are mentioned by references. This thesis, neither in whole or in part, has been previously submitted for any degree.

The work was done under the supervision of Dr. Khawla Qamhieh, at Al – Quds University, Palestine.

Azzam Ali Abu khalil

Acknowledgements

I would like to thank my supervisor Dr. Khawla Qamhieh for her support, encouragement and for providing me this opportunity to acquire the knowledge and expertise in the field of research. Thanks and appreciation to my committe Dr. Mohammad Abu-Ja´far (external examiner) and Prof. Dr. Mohammad Abu-Samreh (internal examiner).

My gratitude also goes to the technician Eng. Mohammad Bawatneh for his assistance in representation some of the theoretical results by a 3-D drawing program.

My thanks extend to my family, friends, who stood beside me and encouraged me constantly.

Finally, I wish to express my gratitude to the Almighty Allah for providing the grant to make this thesis possible.

Azzam Ali Abu khalil

Abstract

The complex formation between the Poly(amido amine) (PAMAM) dendrimer and Deoxyribonucleic acid (DNA) has been studied using a new developed theoretical model describing the interaction between linear polyelectrolyte (LPE) chain and ion – penetrable sphere (Porous sphere) representing dendrimer of different generations G1, G2, G3, G4, G6 and G8. The electrostatic interaction free energy for a system of LPE chain and an oppositely charged sphere has been studied by the penetrable sphere model. The calculated electrostatic interaction free energy is compared with each term calculated by Schiessel model. It was found that the wrapping degree of LPE around dendrimer increases by increasing the concentration of 1:1 salt solution, Bjerrum length and the LPE chain length, as a result the charge inversion of dendrimer becomes stronger. While the wrapping degree decreases by increasing the persistence length of LPE chain (chain rigidity). The aggregate formed by the complexation between a multiple dendrimers and LPE chain bears a slightly constant charge which is negative for all generations with the exception of G4 which found to have a slightly constant and positive net charge when the dendrimer radius is decreased during the interaction between dendrimer and LPE chain. The wrapping degree of LPE chain around dendrimers of smaller generations G1, G2, G3, and G4 increases considerably with increasing of the salt concentration, whereas for higher generations this wrapping degree is insensitive to concentration of salt which means that the aggregate seems to be neutralized. The developed model has been proved to be a suitable one to describe the complexation between the LPE and the dendrimer.

Table of Contents

List of Tables

List of Figures

List of Abbreviations

DNA	Deoxyribonucleic acid
LPE	Linear Polyelectrolyte
PAMAM	Poly(amido amine)
N_{ch}	Number of the monomers on the chain
Z_{dend}.	Number of functional groups of dendrimer
EDA	Ethylenediamine
Cryo-TEM	Cryo-Transmission electron microscopy
TEM	Transmission electron microscopy
MD	Molecular Dynamic
BD	Brownian Dynamic
CG	Coarse – grained
bp	base – pair
l_{opt}	The optimal wrapping length of chain around dendrimer
l_{iso}	The length of the chain needed to neutralized the charge of dendrimer
DLS	Dynamic light scattering
l_p	The persistence length of LPE chain
CSB	Cockayne Syndrome B protein
AFM	Atomic Force Microscopy
dsDNA	Double strand DNA
ssDNA	Single strand DNA

Chapter One

Introduction

Chapter One

1.1 Introduction

Gene therapy is a promising approach for the treatment of both acquired (*e. g.*, AIDS and cancers) and inherited (cystic fibrosis, hemophilia) diseases which are lacking effective drug treatments (Guinn and Mulherkar, 2008; Atkinson, 2008; Youjin and Jun, 2009). During the last decade many targets of gene therapy have been identified although there is still no satisfactory working vector to deliver genetic materials safety and efficiently in vivo (Rolland, 2005). Gene delivery vectors can be roughly divided into two categories: viral and non-viral, viral vectors are efficient in delivering a gene to the target cells although there are problems related to the safety and large-scale production. Non-viral (*i.e.*, chemical) vectors are attractive because of their lower immunogenicity, greater safety and ease of preparation (Kataoka and Harashima, 2001; Itaka and Kataoka, 2009). In addition, chemical vectors can be formulated via a simple routine pharmaceutical process, and are increasingly used in experiments in vitro, in vivo and in clinical trials (**John Wiley and Sons**, 2011).

In a living organism, DNA is vital for its function and information storage (Zinchenko and Chen, 2006). The practical application of DNA compaction is seen in gene therapy and antisense therapy, DNA needs to be compacted and delivered into the interior of the cell nuclei. Such systems contain polyelectrolytes such as DNA interacting with compact colloids such as proteins (Schiessel, 2003; Arcesi et al., 2007), surfactant micelles (Lindman and Thalberg, 1993; Kwak and Dekker, 1998), cationic liposomes (Wolfert et al., 1996; Lasic et al., 1997; Martin-Herranz et al., 2004) and dendrimers (Tomalia et al., 1990; Bielinska et al., 1999), have been used to transfer DNA into cells. Complexes formed between charged Linear Polyelectrolyte (LPE) and oppositely charged sphere are a common pattern in chemistry, physics, and biology. The electrostatic attraction between the sphere and LPE leads to more or less tightly wrapped polymers conformations, in a cell DNA is wrapped around positive charged protein known as histone and forms the nucleosomes structure. These nucleosomes form higher order structures like beads on a string and produce the chromatin structure (Schiessel, 2003).

DNA compaction by nanoscale objective can help us to understand some of the fundamental questions, namely, how the complex conformation depends on the various system parameters such as charge of the sphere and LPE chain, LPE chain length and sphere diameter and salt concentration of the surrounding medium (Netz and Joanny, 1999). There have been numerous experimental, theoretical, and computer simulations studies on DNA compaction on various nanoscale objects such as dendrimers (Ainalem et al., 2009; Carnerup, et al., 2011; Arcesi et al., 2007; Boroudjerdi et al., 2011; Tian and Ma, 2010; Nandy and Maiti, 2011) they showed that the overcharging phenomena of dendrimer was observed when the length of LPE chain exceeds the length that is needed to neutralize the total charge of dendrimer and the overcharging degree depends on dendrimer generation (size and charge) and salt concentration, also they concluded that the morphology and binding model of dendrimer – LPE chain depends on the generation and this binding model is cooperative. While computer simulation studies reported that the LPE penetrates inside dendrimer and this degree of penetration increases with the dendrimer generation or with increase in the charge ratio. Dendrimer can mimic biological macromolecules such as enzymes, viral protein, antibodies, histone, and polyamine such as spermine and spermidine (Tomalia et al., 1990; Bielinska et al., 1999), as a consequence

dendrimers from stable complexes with DNA and protect DNA against degradation (Wang et al., 2010; Fant et al., 2010), such properties make dendrimer excellent tools for gene delivery (Lee et al., 2005).

1.2 Dendrimers

The word dendrimer is derived from the Greek words dendron ('tree' or 'branch') and meros ('part'). Dendrimers are hyper-branched macromolecules comprising a multifunctional core C, several branching points B, and outer surface moieties O as shown in Figure 1.1. Dendrimer size is classified by 'generation', wherein each generation corresponds to a layer of branching units unlike traditional linear polymer synthesis that produces a mixture of materials ranging in molecular weight. Dendrimers are the product of multistep organic synthesis. This difference means that dendrimers can in theory, but not always in practice, be single chemical entities. An opportunity to control dendrimer size, shape, and surface reactivity has brought these molecules to the forefront of biomedicine and drug delivery in particular.

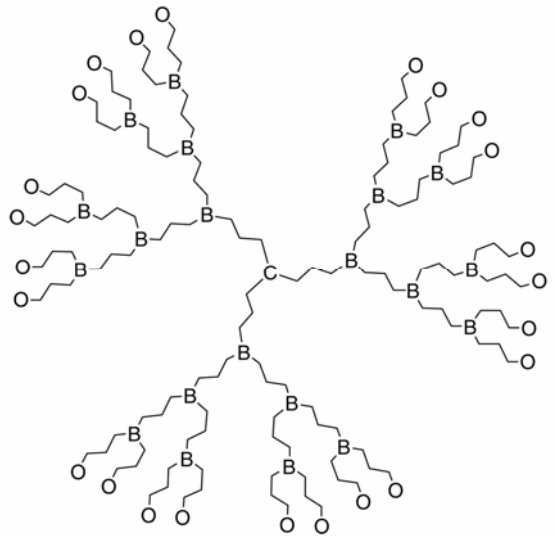

Figure 1.1: Generalized generation dendrimer. C = core, B = branching points, O = outer surface groups.

The dendrimer size linearly increases with every addition of a new branch point (generation, G), and the number of functional primary amine groups (Z) increases exponentially by $Z=N_c N_b^G$, (see Figure 1.2), where N_c represents the core multiplicity (for ethylenediamine $N_c= 4$, and ammonia $N_c= 3$), N_b is the branch cell multiplicity and equals to 2 in both cases, and G is the generation (Tomalia, 2005). *e. g.*, Generation 2 (G2) at neutral pH, has for instance $Z=4\cdot2^2 =16$ surface groups in ethylenediamine cored poly(amido amine) (PAMAM) dendrimer, and $Z=3\cdot2^2=12$ surface groups in ammonia cored PAMAM dendrimer. Table 1.1 shows the number of surface groups for (G0 - G10).

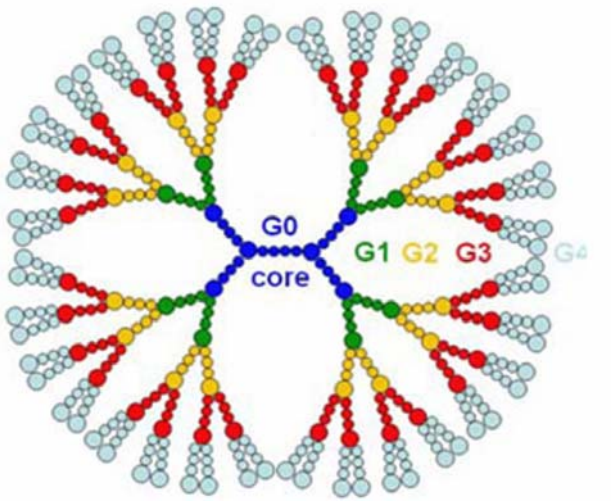

Figure 1.2: Schematic representation of the dendrimer architecture for the case of a tetrafunctional core N_c = 4 and bifunctional branches N_b = 2.

Table 1.1: Theoretical properties of PAMAM dendrimers.

Generation	Number of terminal groups	
	Ammonia cored PAMAM dendrimer	Ethylenediamine cored PAMAM dendrimer
0	3	4
1	6	8
2	12	16
3	24	32
4	48	64
5	96	128
6	192	256
7	384	512
8	768	1024
9	1536	2048
10	3072	4096

The interest in dendrimers is mainly based on their potential applications in various fields ranging from materials engineering to biomedicine and pharmacy. To name but a few, dendrimers have been used to deliver oligonucleotides to the cell (Delong et al., 1997; Yoo et al., 1999). They enhance cytosolic and nuclear availability as indicated by Confocal microscopy as well as cell uptake and transfection efficiency of plasmid DNA (Kukowska -Latallo et al., 1996).

1.2.1 Properties of dendrimers:

1.2.1.1 Monodispersity and Polyvalency:

Dendrimers are dendritic polymers that can be constructed with a well-defined molecular structure, *i.e.*, being monodisperse, unlike the linear polymers. The monodispersity of dendrimer has been extensively verified by gel electrophoresis and transmission electron microscopy (TEM) (Jackson et al., 1998). The convergent growth process permits the purification process at each step of the synthesis which gives the monodisperes molecules. That is the reason, Tomalia said that convergently produced dendrimers are probably the most precise synthetic macromolecules that exist today (Tomalia, 2005). However divergent method is remarkably monodisperse for generation (G = 0 – 5) (Tomalia, 1993). Monodispersity offers researchers the possibility to work with well-defined scalable sizes. This property is useful for applications such as the synthesis of container molecules. Polyvalency of dendrimers provides many interactions as they coordinate to materials. Polyvalency shows the outward presentation of reactive groups on the dendrimer nanostructure exterior, dendrimer's polyvalent depend upon which functional groups are attached to the tip of a dendrimer's branches, these functional groups can participate in multiple interaction with receptors on biological structures like cell membranes and viruses (Halford, 2005).

1.2.1.2 Nanoscale size and shape:

Dendrimers are referred an artificial proteins (Svenson and Tomalia, 2005). Within the PAMAM dendrimer family, the diameter of the generation (G1– G10) with ethylenediamine core increases from 1.1–12.4 nm (Cheng et al., 2008). The shape of dendrimer is very important, as it allows the defined placement of functions not only on dendrimer surface but also inside the dendritic scaffold. The PAMAM dendrimer of lower generation (G0–G3) with ethylenediamine core have ellipsoidal shapes, whereas the PAMAM dendrimer of higher generation (G4–G10) have roughly spherical shapes (Cheng et al., 2008).

1.2.2 Applications of dendrimers:

The ability to deliver pieces of DNA to the required parts of a cell is a challenge. Current research is being performed to find ways to use dendrimers to deliver genes into cells without damaging DNA, also to maintain the activity of DNA during dehydration. Since their introduction in the mid-1980s, this class of dendrimer architecture has been a prime candidate for host guest chemistry (Tomalia et al., 1990). The use of dendrimers as uni-molecular micelles was proposed by Newkome in 1985 (Newkome et al., 1985). This analogy highlighted the utility of dendrimers as solubilizing agents since the majority of drugs available in pharmaceutical industry are hydrophobic in nature and this property in particular creates major formulation problems, dendrimer can be used as drug delivery (Prajapati et al., 2009) and target specific carrier (Kukowska-Latallo et al., 2005). Dendrimers have been used for the encapsulation of hydrophobic compounds and for the delivery of anticancer drugs. Dendrimer may used as drug delivery either the drug is coordinated to the outer functional groups via ionic interactions, or the dendrimer encapsulate a pharmaceutical drug and this encapsulation increase with dendrimer generation.

1.3 General characteristics of DNA

The most important and most abundant form in which DNA can be found in nature is the double-helical B-form as it shown in Figure 1.3.a (Watson and Crick, 1953). In this conformation, the highly negatively charged, Water-soluble double helices have a diameter of about 2.0nm (Mandelkern et al.,, 1981) and can reach gigantic lengths up to several meters, the persistence length of the semi-flexible polymer chains is in the range of (30 – 100) nm (Smith et al., 1992), in eukaryotic cells.

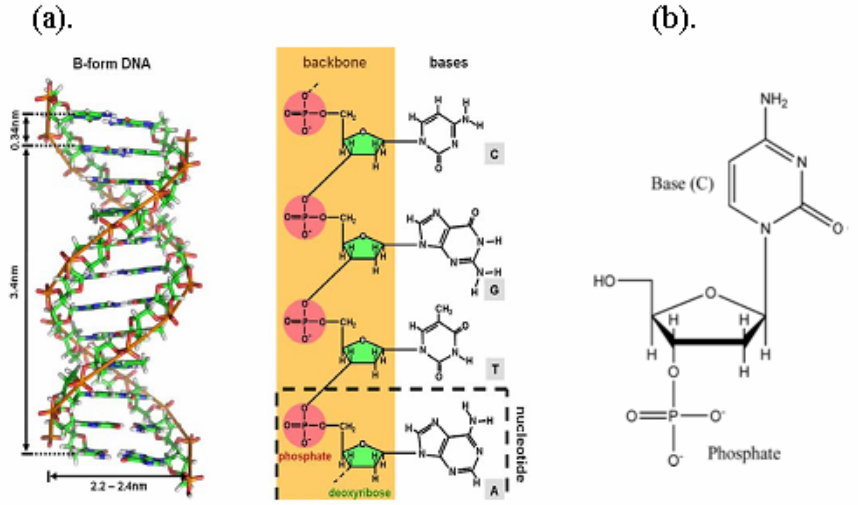

Figure 1.3: (a) Structure and dimensions of B-form DNA, (b) Structure of a nucleotide.

The double helix consists of two tightly associated polymer chains, each being a string of four interchangeable types of basic repeating units called nucleotides (see Figure 1.3.b). Each nucleotide unit contains a sugar-phosphate backbone element, which carries one negative charge. Attached to each sugar is one of four types of bases. These bases are classified into two types: cytosine (C) and thymine (T) are six-membered heterocyclic, organic compounds called pyrimidines (see Figure 1.4.a), while adenine (A) and guanine (G) are fused five- and six-membered rings called purines (see Figure 1.4.b). The length of each DNA backbone unit is about 0.34nm (Mandelkern et al., 1981). The DNA double helix is mainly stabilized by hydrogen bonds between complementary bases on opposite strands forming base pairs (bp), which lie horizontally between the two spiraling strands. Adenine (A) forms a base pair with thymine (T), as guanine (G) does with cytosine (C) in DNA (Watson and Crick, 1953).

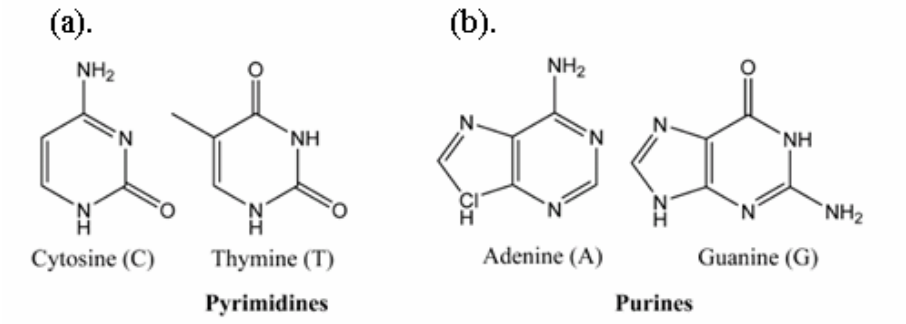

Figure 1.4: Major pyrimidine and purine bases of nucleic acids.

1.3.1 Importance of charge inversion:

To deliver a LPE chain such as DNA from outside to the living cell, the charge of the DNA has to be screened or inverted, because the cell membrane possesses the potential of the same sign as DNA, which prevents the penetration of the DNA through the cell membrane if it is not overcharged, DNA has to be overcharged via complexation with oppositely charged macroion to penetrate through the membrane. As a vehicle for DNA such objects as proteins, dendrimers, micelles, etc. can be used. The formation of complexes DNA - cationic liposomes, when the nucleic acids are completely encapsulated within the positively charged lipid bilayers, is another example of the overcharging (Lasic et al., 1997). Around 90% of the negative charges on the DNA need to be neutralized in order to overcome the intramolecular electrostatics repulsion (Bloomfield, 1997), for this reason the cationic nature of the condensing agents is important in order to decreases the repulsion between the anionic phosphate groups of the DNA backbone, allowing condensation to occur.

1.4 PAMAM dendrimers

PAMAM dendrimers, attract great attention nowadays. Due to their exceptional architecture, monodispersity, low toxicity and high positive charge. Such these vectors are characterized with respect to their ability to neutralize, bind and compact DNA. Because cell membrane is negatively charged, the net positive charge of the PAMAM dendrimer – DNA complex determines the transfection efficiency. Another important aspect for gene therapy is that the bound DNA should be protected from in vivo degradation by the delivery vector. Using Atomic Force Microscopy (AFM) technique, Hosam and co-workers (Hosam et al., 2003) demonstrated that DNA delivered using the PAMAM dendrimer is protected from such degradation. Another advantage of using PAMAM is better transfection efficiency compared with other delivery materials.

1.4.1 Synthesis of PAMAM dendrimers:

Dendrimer can be synthesized to have different functionality in each of these portions to control properties such as solubility, and attachment of compounds for particular applications, synthetic processes can also precisely control the size and number of branches on the dendrimer. There are two defined methods of dendrimer synthesis, divergent synthesis and convergent synthesis. However, because the actual reactions consist of many steps needed to protect the active site, it is difficult to synthesize dendrimers using either method. This makes dendrimers hard to make and very expensive to purchase. At this time, there are only a few companies that sell dendrimers; polymer Factory Sweden AB commercializes biocompatible bis-MPA dendrimers and Dendritech is the only kilogram-scale producers of PAMAM dendrimers. Dendritic Nanotechnologies Inc., from Mount Pleasant, Michigan, USA produces PAMAM dendrimers and other proprietary dendrimers.

In divergent method the dendrimer is assembled from a multifunctional core, which is extended outward by a series of reactions. Each step of the reaction must be driven to full completion to prevent mistakes in the dendrimer, which can cause trailing generations (some branches are shorter than the others). Such impurities can impact the functionality and symmetry of the dendrimer, but are extremely difficult to purify out because the

relative size difference between perfect and imperfect dendrimers is very small (see Figure 1.5).

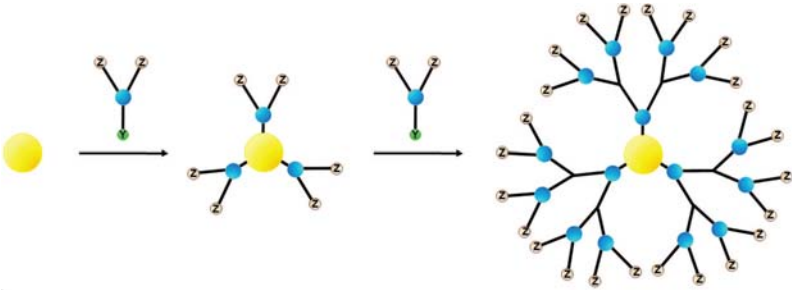

Figure 1.5: Schematic drawing showing the divergent method for synthesis of dendrimers. It starts with a multifunctional initiator core (yellow) that reacts with the chemically activated focal point (Y) of a branched monomer (blue) to produce the first-generation dendrimer. Higher generations are synthesized by the iterative addition of the branched monomers, producing a complete dendrimer terminated with functional chemical groups (Z).

Whereas in convergent method dendrimers are built from small molecules that end up at the surface of the sphere, and reactions precede inward building inward and are eventually attached to a core (see Figure 1.6). This method makes it much easier to remove impurities and shorter branches along the way, so that the final dendrimer is more monodisperse.

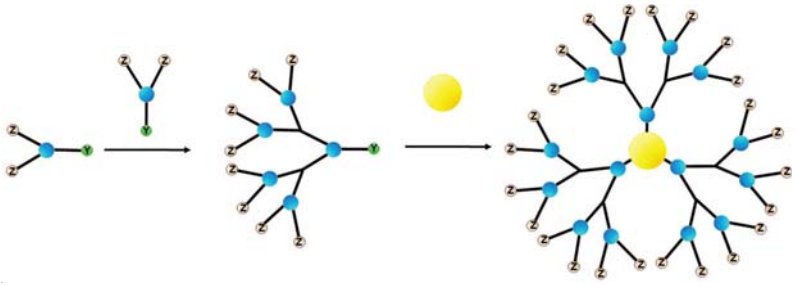

Figure 1.6: Schematic drawing showing the convergent method for synthesis of dendrimers. The dendrimer surface is formed by reaction of the chemically active focal point (Y) of the branched monomer to the functional groups (Z) of another monomer. Dendrons grow by iterative coupling of monomer units to the parent dendron until the desirable dendron size is reached followed by coupling the dendron's focal point to a multifunctional initiator core (yellow) to produce the complete dendrimer.

1.4.2 LPE chain compaction by PAMAM dendrimer

Depending on the size of the nanoscale object and the rigidity of the LPE chain, two mechanisms of LPE chain compaction are usually found: the LPE either is freely adsorbed on the nanoscale objects or forms beads on a string-like object. Deoxyribonucleic acid (DNA) condensation in vitro has attracted considerable attention due to the possibilities within non-viral gene delivery system (Luo and Saltzman, 2000; Kabanov et al., 2000). In eukaryotic organisms, histone proteins are responsible for the packing of DNA within the nucleus, and therefore involved in the control of the genetic activity.

1.4.3 pH dependence of PAMAM dendrimer conformation and DNA-Dendrimer complexation:

To high pH values, all amino groups of PAMAM dendrimers are deprotonated and the dendrimers are uncharged. This results in an increased tendency of the terminal units to fold back into the dendrimer interior leading to a dense-core conformation and smaller radii. In a first protonation step, primary amines of the outer layer of the PAMAM dendrimer protonate independently (Cakara et al., 2003; Niu et al., 2003). The result is a stable conformation with all primary amines protonated and all tertiary amines deprotonated. The arising electrostatic repulsion between like-charged end groups reduces back folding of dendrimer branches and leads to the increase in radius with reducing pH, lowering the pH of the solution further, PAMAM tertiary amino groups protonate (Cakara et al., 2003). This process leads to a stable state, where all amino groups are protonated (see Figure 1.7), with the exception of one central tertiary amino group. As a consequence of increased resulting intra-polymeric coulomb repulsions, dendrimer branches are further extended.

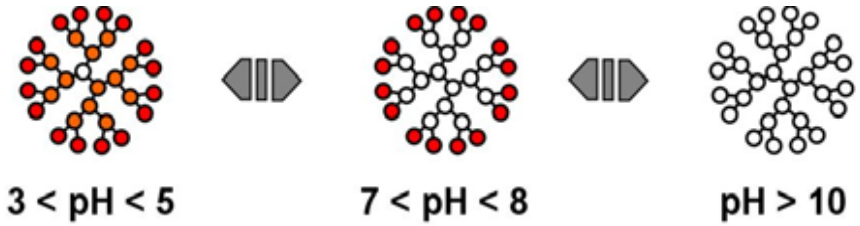

Figure 1.7: Schematic representation of the microscopic protonation mechanism for PAMAM dendrimer.

A recent experimental study (Dootz, et al., 2011) shows the effect of pH values on PAMAM G6 such as radius, total charge, and contributions of primary and tertiary amino groups as shown in Table 1.2.

Table 1.2: Characteristics of PAMAM G6 dendrimer at pH = 5.5 and pH = 8.5.

pH value	Radius(nm)	Contribution of primary amino groups	Contribution of tertiary amino groups	Total charge
5.5	3.55	256e	149e	405e
8.5	3.04	160e	0	160e

At high pH (pH >10) the dendrimer is uncharged and the formation of any DNA-dendrimer complex is not formed, At neutral pH, when the dendrimer is positively charged due to the protonation of all the primary amines, the strong electrostatics interaction helps the DNA strand collapse onto the dendrimer (see Figure 1.8). This electrostatic attraction is resisted by the elastic energy of the DNA due to bending. And when the electrostatic energy overcomes the elastic energy of bending the collapse of the DNA onto dendrimer exists. At neutral pH there is less penetration of DNA compared to at low pH. This implies that at low pH when the complex is formed too much of DNA penetration may complicate its release and thus making its use as gene therapy material difficult (see Figure 1.9). Nevertheless, at low pH condition may be better suited for the purpose of the DNA

delivery inside cell since larger fraction of DNA wrapped around dendrimer and therefore protected. However, if electrostatics interaction is the only major driving force in the DNA wrapping process, then lowering the solution pH further (which increase the dendrimer - DNA charge ratio), should accelerate the wrapping, as various recent experiments have proposed (Luo et al., 2002).

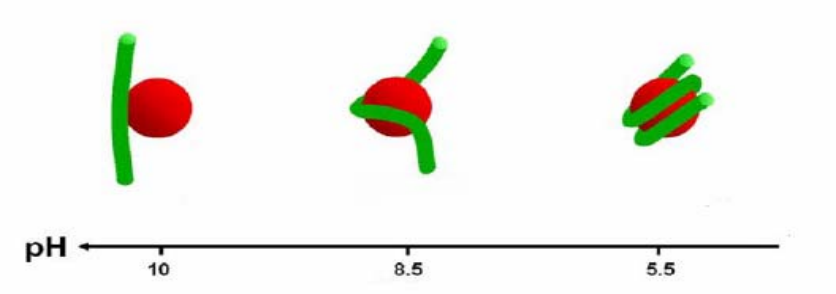

Figure 1.8: Schematic representation of the different conformations of PAMAM dendrimer /DNA complex structures in dependence of the pH controlled dendrimer surface charge density.

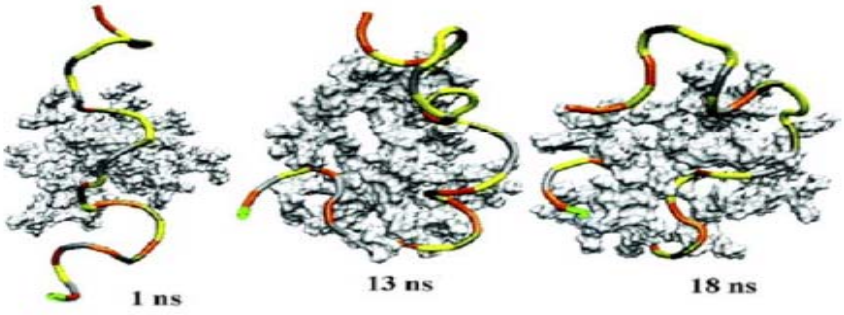

Figure 1.9: Snapshots every few ns of formation of DNA-dendrimer complex (Maiti and Bagchi, 2006).

1.4.4 Wrapping degree of LPE chain around PAMAM dendrimer and Thermodynamics of the Complexation:

Electrostatic interaction is the major binding force for the DNA-dendrimer in the complex (Fant et al., 2008). Molecular dynamics (MD) simulations reveal that it takes first few nanoseconds for the DNA to form stable complex with the dendrimer. Afterward, DNA engages to overcome different energetic hindrances and finds its optimal binding pattern on the dendrimer surface. A recent experiment study of DNA-dendrimer complexation (Fant et al., 2008) suggests that DNA binding with dendrimers can be divided into a "tightly bound DNA" region and a "linker DNA" region. The number of turns of DNA around dendrimer is maximum for the higher dendrimer generations, *i.e.*, the charge ratio between the dendrimer and DNA is maximum. On the other hand, with lower dendrimer generations, *i.e.*, with decreasing charge ratio, the number of turns of DNA around dendrimer decreases. Figure 1.10 shows the effect of generation on the number of attached monomers (number of contacts) on dendrimer (Nandy and Maiti, 20

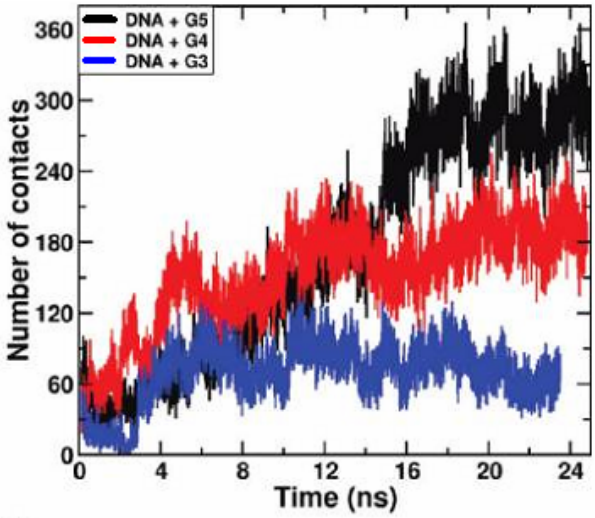

Figure 1.10: The number of attached monomers of DNA on dendrimer as a function of simulation time (Nandy and Maiti, 2011).

When DNA is mixed with PAMAM dendrimers in electrolyte solution, it undergoes a transition from a semiflexible coil to a more compact conformation due to the electrostatics interaction present between the cationic dendrimer and the anionic polyelectrolyte (Örberg et al., 2007). A recent molecular dynamics simulation showed that despite the DNA rigidity, strong electrostatic interactions cause linear DNA chains to wrap around the dendrimer and penetrate inside it, leading to formation of a compact complex (Lee and Larson, 2009). It is known that, when a cationic polymer almost or completely neutralizes an anionic DNA, the intermolecular interaction is expected to be purely electrostatic.

1.5 Previous studies on PAMAM dendrimer – LPE complexation

1.5.1 Experimental studies of PAMAM dendrimer - LPE complexation:

The binding interaction between salmon sperm DNA of 2000bp (L = 680nm) and PAMAM dendrimers of G4 has been investigated. Results based on dynamic light scattering (DLS) and steady-state fluorescence spectroscopy has made it possible to propose a binding model which is cooperative (Örberg et al., 2007). Figure 1.11 shows the proposed binding model. In recent experimental study carried by using cryo-TEM, dynamic light scattering (DLS) and fluorescence spectroscopy (Ainalem et al., 2009) showed that the morphologies of the aggregate formed between DNA and PAMAM dendrimers of different generations are affected by dendrimer size and charge at low charge ratio ($r_{charge} < 1$) in dilute solution. At such conditions the process is cooperative and well-defined structured aggregates are formed for lower dendrimer generations. The smaller sized dendrimer (G1 and G2), which have a lower total charge per molecules, allow the formation of well-structured rods and toroids. In contrast, globular and less defined aggregates are formed with higher generation dendrimers see Figure 1.12.

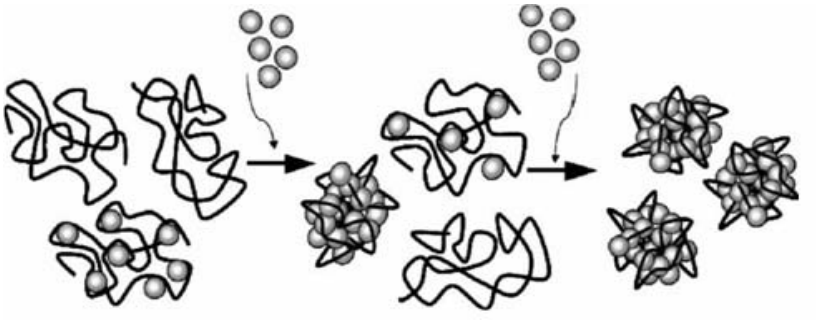

Figure 1.11: The proposed binding model for discrete aggregates formed between DNA and PAMAM dendrimers of generation 4 (Örberg et al., 2007).

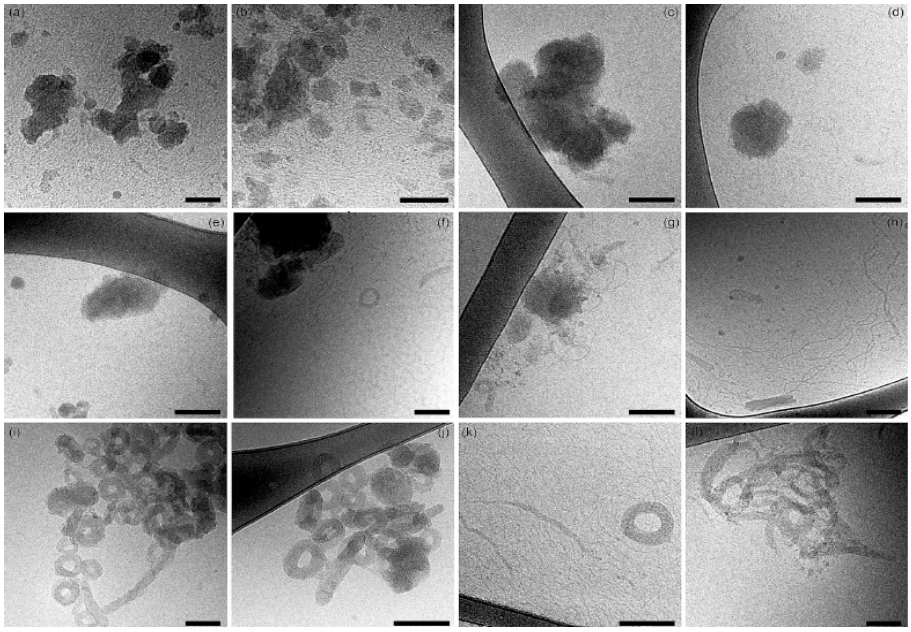

Figure 1.12: Cryo-TEM images of dendrimer/DNA aggregates in 10 mM NaBr where the morphology is seen to vary depending on dendrimer generation displayed is G8/DNA (a, b), G6/DNA (c, d), G4/DNA (e–h), G2/DNA (i, j), and G1/DNA (k, l). Scale bars are 100 nm in all images (Ainalem et al., 2009).

The dendrimer binding to DNA has been also found to be sufficiently strong. For increasing r_{charge} values, the fluorescence emission intensity gradually decreases. This indicates that the amount of free DNA decreases for increased dendrimer concentrations. Ainalem and co-workers assumed that all dendrimers interact with DNA, for low r_{charge} values, the mean resulting numbers of dendrimers per condensed DNA chain of 4331bp are then 318, 16 and 5 for the G2, G6 and G8 of dendrimers respectively. According to the relation $r_{charge} = N_{exp}*Z_{dend}/Z_{DNA}$, these values correspond to mean charge ratios of 0.47 for G2, 0.59 for G6 and 0.61 for G8 (see Table 1.3). The calculated compositions of the dendrimers-DNA aggregate can be compared to the number of 35 for G4 dendrimers that were found per 2000bp (L = 680nm) salmon sperm DNA, which corresponds to a charge ratio of 0.56 in the dendrimer/DNA aggregates.

Table 1.3: Calculated compositions of dendrimer/DNA aggregates using steady state fluorescence spectroscopy for DNA of 4331bp (Ainalem et al., 2009).

Dendrimer generation	Charge ratio	Dendrimers per DNA
G2	0.086	303
	0.13	299
	0.17	305
	0.43	365
G6	0.086	14
	0.13	15
	0.17	16
	0.43	18
G8	0.086	5
	0.13	5
	0.17	5
	0.43	6

.

A recent experimental study performed by Carnerup and co-workers (Carnerup et al., 2011). They studied the condensation of DNA by dendrimer of generations G1, G2, G4, G6, and G8 as a function of salt concentration, and they observed there was an increase in the size of the aggregate formed by lower generations (G1, G2, and G4) when the salt concentration increases. As more rod-like aggregates are observed (see Figure 1.13), whereas for higher generations there was no change in the size *i.e*., such aggregate formed by condensation of DNA by dendrimer of G8 is insensitive to salt concentration. This is attributed to higher charge of higher generation which is more effective to form neutralized aggregates. Figure 1.13 shows the micrographs for different morphologies at salt concentration 150 mM of NaBr compared with Figure 1.12 for salt concentration of 10mM NaBr, both have scale bars of 100 nm.

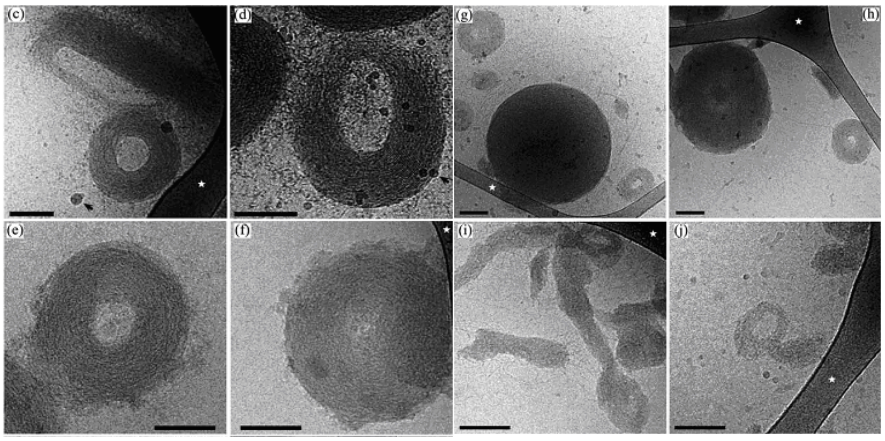

Figure 1.13: Cryo-TEM micrographs of Gx/DNA aggregates condensed in 150 mM NaBr: (c–d) G1/DNA, (e and f) G2/DNA, (g and h) G4/DNA and (i and j) G6/DNA compared to Figure 1.12 at 10 mM NaBr. Scale bars are 100 nm in all images (Carnerup et al., 2011).

1.5.2 Computer simulation studies of PAMAM dendrimer - LPE complexation:

The complexation of a PAMAM dendrimer with an oppositely charged LPE has been motivated many simulation studies aimed at understand the atomistic details of the process. Luylin and co-workers (Luylin et al., 2005) performed Brownian dynamics computer simulations of complexes formed by charged dendrimer and oppositely charged linear polymer chain of different degree of polymerization (different number of monomers on the chain N_{ch}). They showed that when the monomers of the linear chains with N_{ch} equal to number of dendrimer's terminal charged groups are located very close to these terminal groups. For longer chains the total number of the chain monomers adsorbed onto a dendrimer exceeds the number that is necessary to neutralize dendrimer´s charge. The overcharging phenomenon was observed.

A recent MD simulation study, Luylin and co-workers (Luylin et al., 2008), showed that the maximum of the LPE chain adsorption occurs at some critical length of LPE chain. The first order phase transition from completely coiled conformation to the conformation with released tails takes place upon increasing the linear-chain length above the critical length. The one-long-tail conformation becomes energetically preferable. Larin and co-workers (Larin et al., 2009) studied the structural properties of the complexes formed by two macroions and a LPE chain. They found that the dependence of Nonmonotonic of the linker size on the LPE chain length was observed.

More advances in molecular dynamics simulation methodologies and computational power performed such as the coarse-grained (CG) simulations. Tian and Ma (Tian and Ma, 2010) employed extensive coarse – grained molecular dynamic simulation to study the influence of rigidity of the LPE chain on dendrimer – LPE complexes. They found that as a soft nanoparticle. The change in size and shape of dendrimer depends on the Bjerrum length of the medium and the condensed LPE chain monomers have additional possibility for the localization near the opposite charge inside the layer.

1.6 Theoretical models

The first theoretical models on sphere – LPE chain complexation were presented in 1999. Park and co-workers (Park et al., 1999) considered a semiflexible and highly charged PE chain and showed that counterion release leads to overcharging. Mateescu and co-workers (Mateescu et al., 1999) considered the interaction between a spherical macroion of charge Ze and an oppositely, highly charged polyelectrolyte of charge $-Ne$. They showed that, for $N > Z$, the amount of collapsed polyelectrolyte can be bigger than that required to neutralize the macroion, *i.e.* the macroion can be overcharged. The overcharging increases with the diameter of the macroion. The predictions of this model compared with Monte Carlo Simulations.

Netz and Joanny (Netz and Joanny, 1999) studied the interaction of a charged semiflexible polymer with an oppositely charged hard sphere. Both the effect of salt concentration and the stiffness of the polymer are taken into account. They showed that for intermediate salt concentration and high enough sphere charge a strongly bound complex obtained where the polymer completely wraps around the hard sphere. The complex may or may not exhibit charge reversal, depending on the sphere charge and slat concentration. In the case of low salt the regime is dominated by the polymer-polymer repulsion, the polymer partially wraps around the sphere, and the two polymer arms extended parallel and in

opposite directions from the sphere. Whereas in high salt regime they found bent solution, and the salt dependence of the wrapping transition for large salt concentrations agree with experimental results for the complexation of synthetic polyelectrolytes with charged colloids.

Nguyen and Shklovskii (Nguyen and Shklovskii, 2001) studied the complexation of a polyelectrolyte with an oppositely charged spherical macroion modeled impenetrable sphere, for both salt free and salty solutions. They showed when a polyelectrolyte winds around the macroion, its turns repel each other and form an almost equidistant solenoid. Nguyen and Shklovskii concluded that this correlation of turns lead to the charge inversion, and the charge inversion becomes stronger with increasing concentration of the salt, this analytical study agrees with Monte Carlo simulation results.

Schiessel and co-workers (Schiessel et al., 2001) considered complexes formed between positively charged macroion and a persistence LPE. They studied first the case of complexation with a single hard sphere and calculated the wrapping length of the chain. Then they extended their consideration to complexes of many wrapped spheres. (See appendix A).

Schiessel and co-workers showed how the resulting complexes depend on the persistence length of the linear polyelectrolyte, the salt concentration, the size and charges of the chain and the macroions (Schiessel et al., 2001). In the same frame of this analytical study Qamhieh and co-workers (Qamhieh et al., 2009) extended this analytical study of the complexation of highly charged semiflexible LPE modeling DNA with an oppositely charged hard sphere modeled dendrimer of G4. They inserted minor modifications to the model developed by Schiessel. They studied the net charge of the complex conformed by dendrimer of G4 complexes with semiflexible LPE chain of two lengths, and how much the LPE chain wrapped around the dendrimer and the number of dendrimers in the aggregate. Throughout the analytical study, the term (complex) refers to the interaction between a single ion-penetrable sphere representing dendrimer and segment of linear polyelectrolyte (LPE) representing DNA molecule that wrapped around dendrimer. And the term (aggregate) refers to the interaction between a multiple of dendrimers and the whole DNA molecule length as shown in Figure 1.14.

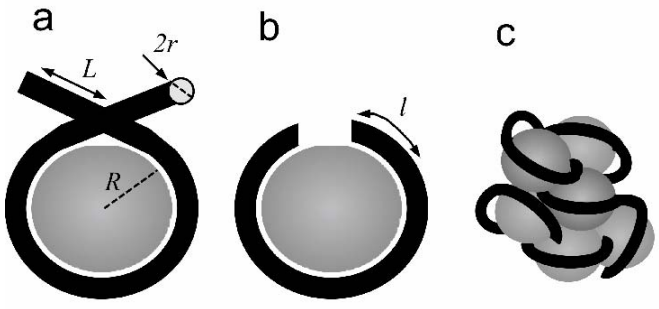

Figure 1.14: Schematic representation of (a) a piece of a DNA molecule is shown to wrap around one dendrimer. The DNA segments linking to the next dendrimer in an aggregate. (b) a dendrimer/DNA complex consisting only of one dendrimer and the DNA segment actually wrapping the dendrimer, *l*. (c) the dendrimer/DNA aggregate consisting of the entire DNA molecule and a multiple of dendrimers (Qamhieh et al., in progress).

They concluded that dendrimers are likely to contract upon interaction with oppositely charged LPE. For this reason Qamhieh and co-workers recommend to replace the complexation of semiflexible LPE chain with impenetrable sphere by a soft sphere.

Qamhieh and co-workers (Qamhieh et al., in progress) extended this analytical study to include the interaction between semiflexible LPE chain and oppositely charged dendrimer of generations G2, G4, G6 and G8. One length of LPE was used 4331bp. They found that the number of turns of LPE around dendrimer increases with dendrimer generation, and the net charge of the aggregates is independent of dendrimer size when it contract especially for higher generation.

1.7 Statement of the problem

In this section, we would like to modify the model developed by Schiessel and co-workers (Schiessel et al., 2001) by replacing the hard sphere by ion-penetrable sphere (see Figure 1.15). Because dendrimers are proved to be fairly flexible and allow penetration of the LPE inside them and this degree of penetration increases with the increase of dendrimer generation or increase in the dendrimer – LPE chain charge ratio. This analytical study has a great practical significance to be an exciting area for further research in gene therapy. It can give us predictions about the net charge, size and other structural properties of the nucleosome formed from the complexation between DNA and dendrimer of different generations. Hence, desired transfection efficiency can be achieved.

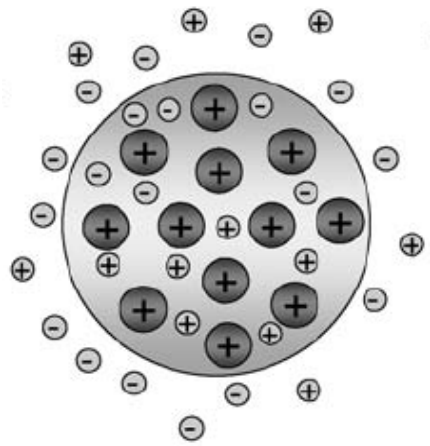

Figure 1.15: Charged ion penetrable spherical particle the large circle with + sign stands for the particle fixed charges, while the small circles with + or – stand for electrolyte cations and anions.

Chapter Two

The Theoretical Model

2.1 Introduction

Many modifications have been made on Schiessel and co-workers model (Schiessel et al., 2001), which describes the interaction between the LPE chain and a multiple hard spheres (see appendix A). Our modifications include the following terms as expressed by Schiessel and co-workers:

1. The electrostatic charging free energy of a spherical complex of charge $Z(l)e$. See Eq. (A.2) in appendix A.
2. The electrostatic free energy of the interaction between the complex and the remainder of the chain (unwrapped part). See Eq. (A.7) in appendix A.
3. The repulsive electrostatic interaction free energy between hard spheres. See Eq. (A.10) in appendix A.

2.2 Analytical model of the system

In this analytical study the dendrimer was modeled as a penetrable sphere of radius R and charge Ze. Where the penetrable sphere has a charge distributed through the whole volume not only at the surface as in the case of the hard sphere (impenetrable sphere). The LPE chain was considered as rod of radius a=1nm, and different contour lengths L, where $L>>R$. The charge of the LPE per unit length is $\lambda = -e / b$, where b is the distance between charged monomers on the chain (see Figure 2.1). And a persistence length l_p (Hagerman, 1988) which is large compared to R. Both are placed in a monovalent salt solution characterized by a Bjerrum length $l_B = e^2/\varepsilon k_B T$ (ε: dielectric constant of the medium, T: absolute temperature) and Debye screening length is $\kappa^{-1} = (8c_s\pi l_B)^{-1/2}$ (c_s: Concentration of salt). In this study we will focus on the salt concentration in the medium *i.e.*, κ^{-1} takes different values.

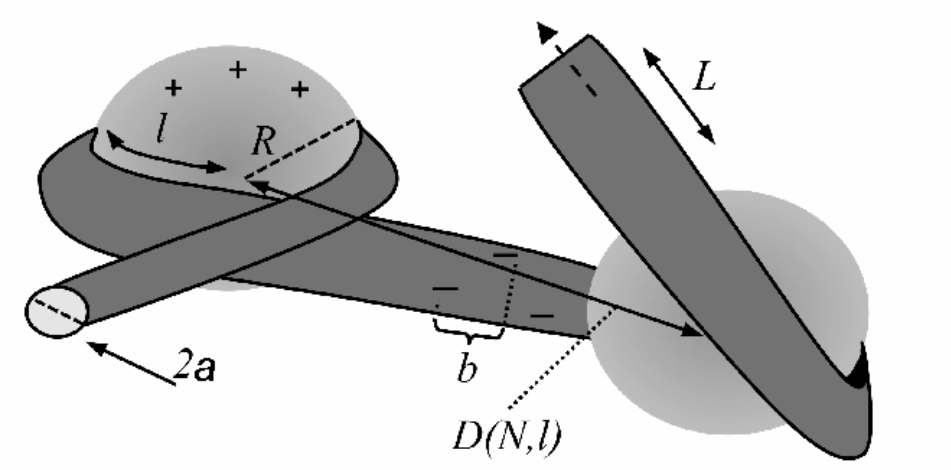

Figure 2.1: The proposed binding model between DNA of contour length L, radius a, and distance between negative charges b and Gx PAMAM dendrimers modeled as penetrable spheres of radius R. The DNA is shown to wrap around the dendrimer with the length of the wrapping part equal to l, and a distance between the centers of two neighboring dendrimers, $D(N,l)$. The model is in accordance with the cooperative binding model proposed by Örberg on co-workers (Örberg et al., 2007).

2.3 Free energy calculation for a complexation between a PE chain and a single ion-penetrable sphere

For the of LPE chain – penetrable sphere complex, the total free energy can be determined as follows: Assume that a length l of the chain has been wrapped around the sphere and they divided LPE chain – sphere complex in two parts, the chain will wrap around sphere of length l and the remaining chain of the unwrapped length is $(L - l)$.

From the total free energy equation of a single complex formed by the interaction between a single penetrable sphere and LPE chain. Similar to Schiessel model see Eq. (A.1) in appendix A.

$$F(l) = F_{compl}(l) + F_{chain}(L-l) + F_{compl-chain}(l) + F_{elastic}(l) \qquad (2.1)$$

These modifications include the first and third term in Eq. (2.1) which represent the charging free energy of the complex of charge $Z(l)e$ and the interaction free energy between the complex and the free chain of un-wrapped length of $(L-l)$ respectively.

According to Ohshima (see Eq. (B.22) in appendix B) the electrostatic charging free energy of weakly charged ion-penetrable sphere of charge Ze (Ohshima et al., 1993) is given by:

$$F_{sphere}(Z) \cong \frac{3Z^2e^2}{8\pi\varepsilon(\kappa R)^2}\left[\cosh(\kappa R) - \frac{\sinh(\kappa R)}{\kappa R}\right]\frac{e^{-\kappa R}}{R} \qquad (2.2)$$

The total charges of the complex of wrapped length l of LPE chain can be expressed by

$$Z(l)e = (Z - l/b)e \qquad (2.3)$$

Thus, we can write the electrostatic charging free energy of a spherical complex of charge $Z(l)e$, by using Bjerrum length (Bjerrum, 1959).

$$l_B = \frac{e^2}{\varepsilon k_B T} \quad (\mathrm{c}^2/\mathrm{Joule}) \qquad (2.4)$$

We can get:

$$F_{compl}(l) \cong \frac{3Z^2(l)l_B k_B T}{8\pi(\kappa R)^2}\left[\cosh(\kappa R) - \frac{\sinh(\kappa R)}{\kappa R}\right]\frac{e^{-\kappa R}}{R} \qquad (2.5)$$

Eq. (2.5) implies that $F_{compl}(l)$ varies quadratically as $(Z - l/b)^2$. There is special length $l_{iso} = bZ$ such that $Z(l = l_{iso}) = 0$. Simply invoking the principle of charge neutrality would lead to expect that the total free energy is minimized for $l \approx l_{iso}$, where l_{iso} is the isoelectric chain length needed to compensate the charge of the porous sphere.

The second term in Eq. (2.1) is the total entropic free energy of the remaining chain of length (*L-l*) form Schiessel model (see Eq. (A.4) in appendix A)

$$F_{chain}(L-l) \cong \frac{k_B T}{b} \cdot \Omega(a) \cdot (L-l) \tag{2.6}$$

Where $\Omega(a)$, is the entropic cost to confine counterions close to chain given by

$$\Omega(a) \cong 2\ln\left(\frac{4\xi\kappa^{-1}}{a}\right) \tag{2.7}$$

Schiessel and co-workers restricted their study of the complexation between LPE chain and hard sphere to highly charged LPE chain *i.e.*, the distance between charges on the chain is much smaller than Bjerrum length, where the so called manning parameter $\xi = l_B / b$; $\xi >> 1$, according to Manning (Manning, 1978); they ignored ξ^{-1} in their study. Here, the monomer spacer b = 0.7 nm which is comparable with Bjerrum length at room temperature. Thus, ξ^{-1} is taken explicitly into account in our analytical study. Hence, Eq. (2.6) can be expressed as

$$F_{chain}(L-l) \cong \frac{k_B T}{b} \cdot \Omega(a) \cdot (L-l) \cdot (1-\xi^{-1}) \tag{2.8}$$

The third term, $F_{compl\text{-}chain}(l)$ in Eq. (2.1), is the electrostatic free energy of the interaction between the complex and the remainder of the chain of length (*L-l*), given by

$$dF_{compl-chain}(l) \cong \varphi_{compl} \cdot dq_{chain} \tag{2.9}$$

Where q_{chain} is the charge of the unwrapped length of PE around the penetrable sphere (*L-l*), it can be written as the following

$$dq_{chain} = \lambda_{chain} \cdot dr \tag{2.10}$$

The electric potential of the sphere of charge *Ze* is earlier obtained by Ohshima (see Eq. (B.18) in appendix B), to express the electric potential for a spherical complex of charge $Z(l)e$, just we need to replace the charge of sphere Z by $Z(l)$, we get

$$\varphi_{compl}(l) \cong \frac{3Z(l)e}{4\pi\varepsilon(\kappa R)^2}\left[\cosh(\kappa R) - \frac{\sinh(\kappa R)}{\kappa R}\right]\frac{e^{-\kappa r}}{r} \tag{2.11}$$

Substituting Eq. (2.11) and Eq. (2.10) into Eq. (2.9) we get:

$$dF_{compl-chain}(l) \cong \frac{3Z(l)e}{4\pi\varepsilon(\kappa R)^2}\frac{e^{-\kappa r}}{r}\left[\cosh(\kappa R) - \frac{\sinh(\kappa R)}{\kappa R}\right]$$
$$\lambda_{compl} \times dr \tag{2.12}$$

By using the linear charge density of the PE chain and substituting it into Eq. (2.12) we can get:

$$dF_{compl-chain}(l) \cong \frac{3Z(l)e^2}{4\pi\varepsilon(\kappa R)^2}\frac{e^{-\kappa r}}{r}\left[\cosh(\kappa R)-\frac{\sinh(\kappa R)}{\kappa R}\right]\frac{dr}{b} \quad (2.13)$$

Taking the integration of the free energy then

$$F_{compl-chain}(l) \cong \frac{3Z(l)e^2}{4b\pi\varepsilon(\kappa R)^2}\left[\cosh(\kappa R)-\frac{\sinh(\kappa R)}{\kappa R}\right]\int_R^{L-l}\frac{e^{-\kappa r}}{r}dr \quad (2.14)$$

The resulting free energy between the complex and the unwrapped segment of the PE chain is given by

$$F_{compl-chain}(l) \cong \frac{3Z(l)l_B k_B T}{4\pi(\kappa R)^2}\left[\cosh(\kappa R)-\frac{\sinh(\kappa R)}{\kappa R}\right]$$
$$\times\left[\ln(r)-\sum_{n=0}^{\infty}\frac{(-1)^n}{(\mathrm{n}+1)!\cdot(\mathrm{n}+1)}\cdot(\kappa r)^{n+1}\right]\Bigg|_R^{L-l} \quad (2.15)$$

The final term in Eq. (2.1), $F_{elastic}(l)$, is the elastic (bending) free energy required to bend l of the chain of radius of curvature around sphere of radius R is the same as the one used in Schiessel model (see Eq. (A.8) in appendix A).

$$F_{elastic}(l) \cong \frac{k_B T l_p}{2R^2}l \quad (2.16)$$

2.4 Free energy calculation for the complexation of a chain with multiple spheres

The total free energy for a system consisting of one LPE chain and N number of spheres (see Eq. (A.9) in appendix A) can be expressed as

$$F(l,N) = NF(l) + F_{\mathrm{int}}(N,l) \quad (2.17)$$

The second term in Eq. (2.17) which represents the repulsive electrostatic interaction free energy between hard spheres. Also, this term has to be modified to represent the electrostatic interaction free energy between penetrable spheres.

Ohshima found the electrostatic interaction free energy between two ion – penetrable spheres (see Eq. (B.28) in appendix B). Each of charge Ze as following:

$$F_{\mathrm{int}} = \frac{9Z^2e^2}{8\pi\ \varepsilon(\kappa R)^4}\left[\cosh(\kappa R)-\frac{\sinh(\kappa R)}{\kappa R}\right]^2\frac{e^{-\kappa D}}{D} \quad (2.18)$$

For the case of the interaction between complexes each of charge $Z(l)e$, by using Eqs. (2.3), (2.4) and (2.18). Then, the interaction free energy can be obtained by summing over the electrostatic repulsion between all complexes within one chain. We get

$$F_{\text{int}}(N,l) = \frac{9Z^2(l)k_BTl_B}{8\pi(\kappa R)^4}\left[\cosh(\kappa R) - \frac{\sinh(\kappa R)}{\kappa R}\right]^2$$
$$\times \sum_{i=1}^{N-1}\left[\left[\frac{N-i}{i}\right]\frac{e^{-\kappa D(N,l)}}{D(N,l)}\right] \qquad (2.19)$$

Where $D(N,l)$ the center-to-center distance between two complexes next to each other which equals to $(L\text{-}Nl+2NR)/N$, is small at very low ionic strength, This interaction energy worths nothing that this term will be small if the charge of complex is close to neutral.

For simplification we write

$$A = \cosh(\kappa R) - \frac{\sinh(\kappa R)}{\kappa R} \qquad (2.20)$$

Substituting Eqs. (2.5), (2.8), (2.14), (2.16) and (2.19) into Eq. (2.17) we get

$$\frac{F(N,l)}{k_BT} = \frac{3NZ(l)l_BA}{4\pi(\kappa R)^2}\left[\frac{Z(l)}{2}\frac{e^{-\kappa R}}{R} + \frac{1}{b}\cdot\int_R^{L-Nl}\frac{e^{-\kappa r}}{r}dr + \frac{3Z(l)A}{2(\kappa R)^2}\sum_{i=1}^{N-1}\left(\frac{N-i}{i}\right)\frac{e^{-\kappa D}}{D}\right]$$
$$+\frac{1}{b}\cdot\Omega(a)\cdot(1-\xi^{-1})\cdot(L-Nl) + \frac{Nl_p}{2R^2}l. \qquad (2.21)$$

Thus, Eq. (2.21) represents the total free energy of the system in units of k_BT. It can be used to investigate the behavior of dendrimer of generations G1 – G8 during its interaction with LPE chain.

Chapter Three

Results and Discussions

Chapter Three

Results and Discussions

3.1 Computational details

The present calculations have been performed using more advanced computational software. In the present work the optimization method (finding minima) of the total free energy for a system of N interacting penetrable spheres with LPE chain of contour length L was done by the essential tool for mathematic and modeling Maple 12, and also we used the Originlab program of version 7.5 for graphing and analyzing some of the theoretical results.

3.2 Results of electrostatic interaction free energy of the complexation between LPE chain and penetrable sphere

The electrostatic interaction free energy for a system of LPE chain and an oppositely charged sphere has been studied by the penetrable sphere model. The LPE chain modeled DNA molecule of 88bp, and penetrable sphere of charge $Z = 64$ and radius $R = 2.25$nm representing PAMAM dendrimer of generation 4 at concentration of 1:1 salt solution NaBr corresponds to Debye screening length of 3nm and Bjerrum length of 0.71nm at room temperature. The calculated electrostatic interaction free energy for this system has been plotted as a function of the wrapping length l individually and compared with each term calculated by Schiessel model (Eqs. (A.1) and (A.10)). Figure 3.1a shows the electrostatic charging free energy of the complex (the first term in Eq. (2.1)) with a total charge of $Z(l)e$ resulting from the wrapping of a finite length of LPE chain around penetrable sphere, it was shown to vary quadratically with the wrapping length. Figure 3.2a shows the electrostatic interaction free energy between the un-wrapped segment of LPE chain of length $(L-l)$ and the complex of charge $Z(l)e$ (the third term in Eq. (2.1)), this free energy is attractive at small wrapping lengths *i.e.*, when $l < l_{iso}$ the complex bears a positive total charge while the LPE chain in its native state is negatively charged, for a large wrapping lengths *i.e.*, $l > l_{iso}$, it becomes repulsive when calculated by our model. Figure 3.3a represents the electrostatic interaction free energy between two complexes of equal total charge of $Z(l)e$ calculated by the penetrable sphere model (see Eq. (2.19)) which is repulsive free energy at any value of the wrapping length , except at $l = l_{iso}$, where at this value the complexes get neutralized.

The calculated charging free energy for both penetrable sphere and hard sphere models follows the same trend with different values, as it shown in Figure 3.1b (the first term in Eq. (A.1) in Schiessel model) which shows a larger value in the calculated charging free energy compared with Figure 3.1a. The value of the interaction free energy calculated by our model (see Figure 3.2a) is larger than that calculated by Schiessel model as shown in Figure 3.2b (the third term in Eq. (A.1)). Figure 3.3a shows a more reasonable correlation between the repulsive free energy between two complexes and the wrapping length compared with the interaction free energy calculated by the hard sphere model as represented in Figure 3.3b (see Eq. (A.10)) this interaction free energy cannot be attractive for all wrapping lengths, if $l = l_{iso}$ the interaction free energy is zero for both hard sphere and penetrable sphere models.
Figure 3.4 summarizes the contributions of these terms namely, the charging free energy of the complex, the interaction free energy between complex and chain and the interaction

free energy between complexes, Figure 3.4a represents the total electrostatic free energy for the penetrable sphere model and Figure 3.4b for hard sphere model. The electrostatic free energy minimized to -26 and -17 each in units of k_BT for the penetrable sphere and hard sphere respectively.

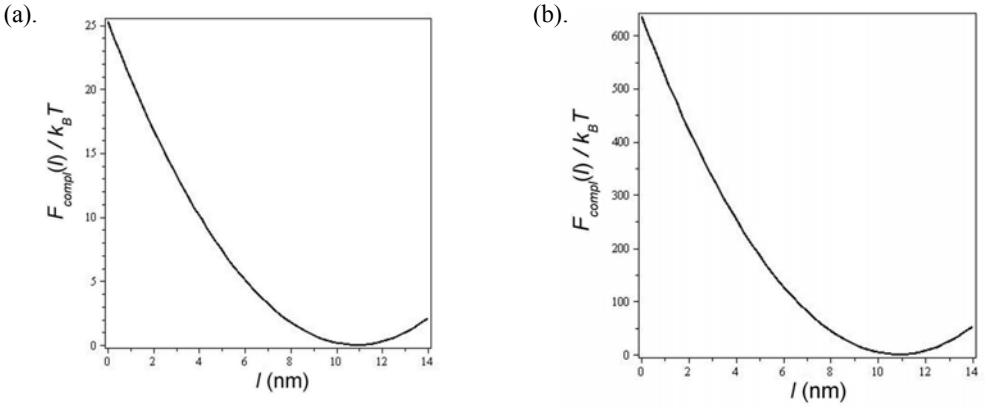

Figure 3.1: Electrostatic charging free energy in units of k_BT of G4 – LPE chain complex as a function of the wrapping length, (a) for penetrable sphere model, and (b) for hard sphere model.

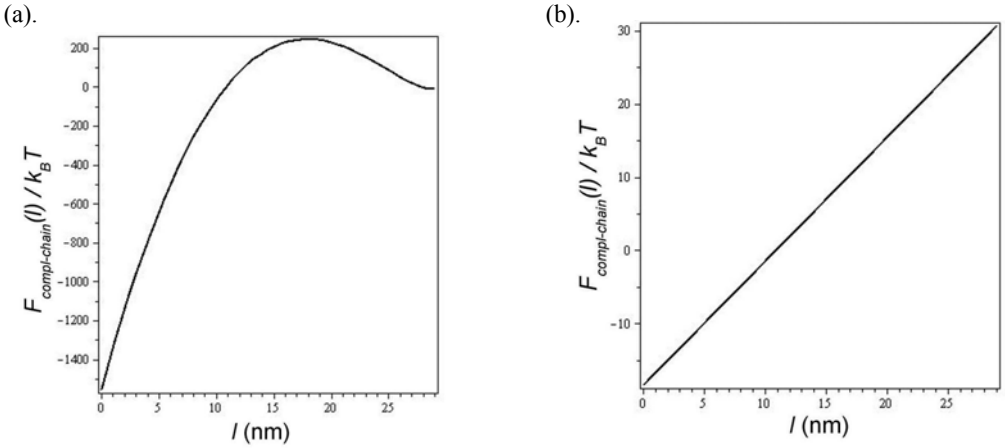

Figure 3.2: Electrostatic interaction free energy in units of k_BT between G4 – LPE chain complex and free chain of length (L-l) as a function of the wrapping length (a) for penetrable sphere model, and (b) hard sphere model.

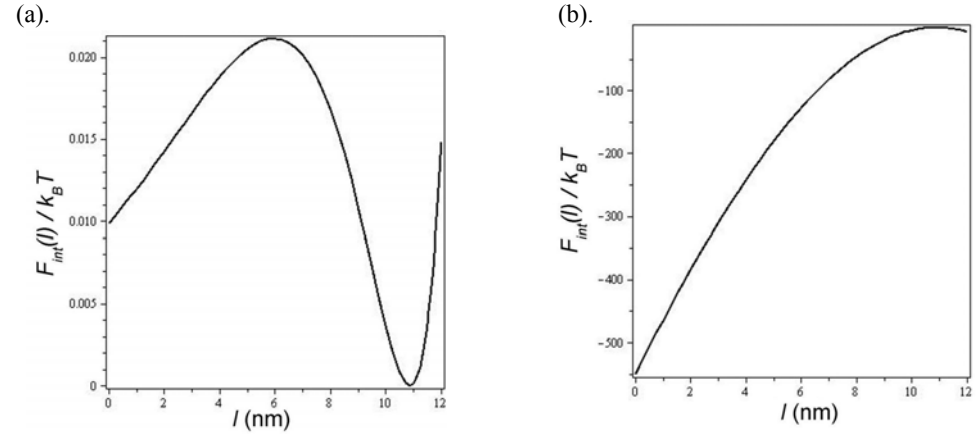

Figure 3.3: Electrostatic interaction free energy in units of k_BT between 2G4 – LPE chain complexes as a function of the wrapping length, for (a) penetrable sphere model, and (b) for hard sphere model.

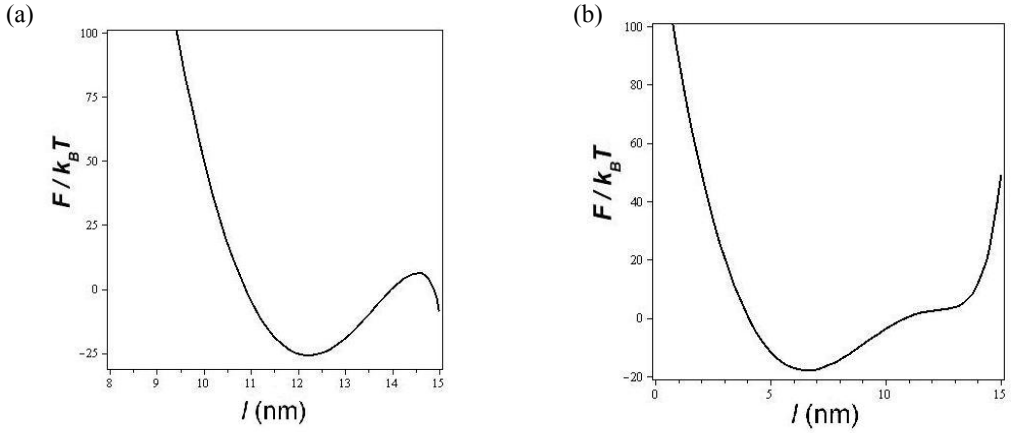

Figure 3.4: The total electrostatic free energy in units of k_BT of 2G4 – LPE chain complexes as a function of the wrapping length, for (a) penetrable sphere model, (b) for hard sphere model.

3.3 Single PAMAM dendrimer – LPE chain complex

For a system of LPE chain and PAMAM dendrimer of different generations, the optimal wrapping length (l_{opt}) of LPE chain which has been wrapped around dendrimer can be found by taking the first derivative of total free energy equation for the penetrable sphere model (Eq. (2.21)) with respect to the wrapping length l, then equating it to zero (*i.e.*, the total free energy equation has to be minimized). Through out this study we have used a quantity measure this wrapping degree of LPE chain around dendrimer namely, the fraction of the condensed monomers of LPE chain each of charge $-e$ on the dendrimer.

The complex conformation by LPE chain and a single dendrimer in a 1:1 salt solution of NaBr has been studied by the penetrable sphere model. Many effects on the complexation have been studied, mention but a few, the effect of salt concentration in the case of 1:1 salt solution, the Bjerrum length in the medium, the dendrimer charge and the influence of the rigidity of the LPE chain (Persistence length).

3.3.1 Effect of Bjerrum length on PAMAM dendrimer – LPE complex conformation:

The flexible LPE chain of persistence length l_p = 3nm was chosen to bear 10 negatively charged monomers (-10e) in the case of monovalent chain (single strand) and 20 negatively charged monomers (-20e) in the case of divalent chain (double strands) of total length 6.7nm. The systems have been studied by the penetrable sphere model at 1:1 salt concentration corresponds to Debye screening length of 6nm. We pointed here that the overall charge of dendrimer which equals to 48 terminal positively charged monomers at physiological conditions exceeds the total charge of the linear polyelectrolyte chain in both cases of monovalent and divalent chain, *i.e.,* the overcharging phenomena of dendrimer will not occur. The fraction of the condensed monomers of the LPE chain each of charge -e on the PAMAM dendrimer of generation 4 and the total charge of the complex are analytically studied for different Bjerrum lengths which measures the strength of the electrostatic attraction between LPE chain and dendrimer complexes. The net charge of the complex can be calculated in terms of $Z_{compl} = Z_{dend} - Z_{cond}$, where Z_{dend} is the total charge of the positively charged dendrimer in the case of ammonia cored PAMAM dendrimer of

G4, and Z_{cond} is the total charge of the chain that condensed on the dendrimer, it can be written in terms of l_{opt} / b.

As it shown in Figure 3.5a for both monovalent and divalent chain, for a weak electrostatic interaction *i.e.*, for small values of Bejrrum length, there is small fraction of the condensed monomers on dendrimer which means that chain tails are the dominant, by increasing the ratio between the Bjerrum length and monomers spacer b, the chain tails disappear very quickly. The calculated maximum fraction of the condensed monomers of the LPE chain by our study was found to reach to 0.86 and 0.95 for monovalent and divalent chains respectively, these results are compared with molecular dynamic simulations which showed a larger fraction of the condensed monomers to reach about 0.99 for both monovalent and divalent chain, both the penetrable sphere model and MD simulations show a saturation in the condensed monomers at the same value of the ratio between the Bjerrum length and the monomers spacer, *i.e.*, at $l_B \geq 3.25b$.

Figures 3.5b shows the total charge of the complex normalized to the total charged monomers of G4 as a function of Bjerrum length in the case of monovalent and divalent chains, it turns out that the divalent chain is more effective in neutralizing charged dendrimer, as a result, we showed that a reduction in the normalized charge of the complex from 0.90 to 0.82 for monovalent chain and from 0.65 to 0.60 for divalent chain, while MD simulations showed a reduction from 0.82 to 0.79, and from 0.60 to 0.59. The effect of Bjerrum length on the fraction of the condensed monomers and the normalized charge of the complex is also studied by the hard sphere model developed by Shciessel.

Figure 3.6a represents the fraction of the condensed monomers of the LPE chain, for small values of Bjerrum length we get negative values of the LPE wrapping length for both monovalent and divalent chain which is not reasonable results, also the fraction of the condensed monomers in the case of divalent chain exceeds the unity. Figure 3.6b shows the normalized charge of the complex to dendrimer charge, the ratio between the complex total charge and dendrimer charge is larger than one at small values of Bjerrum length for both monovalent and divalent chain and this is impossible. So, the results obtained by the hard sphere model are away to be compared to MD simulations. We didn't take explicitly into account the effect of counterions on the complex conformation in our theoretical study as Lyulin and co-workers in their study (Lyulin et al., 2008).

Figure 3.7 shows the charge of the counterions condensed on G4 – LPE chain complex normalized to dendrimer charge as a function of Bjerrum length, as it shown the average fraction increase with the increasing of Bjerrum length and this fraction of the condensed counterions on the G4 – LPE complex in the case of the complexation of dendrimer with monovalent chain is larger than that of the complexation of dendrimer with divalent chain and this can be explained by the fact that the divalent chain is more effective in neutralizing dendrimer charge.

(a)

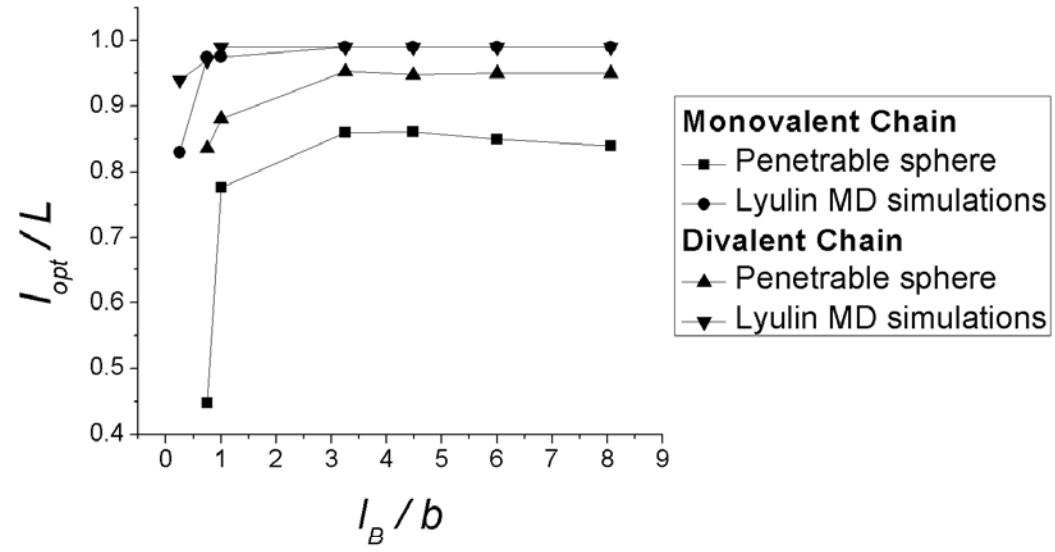

(b)

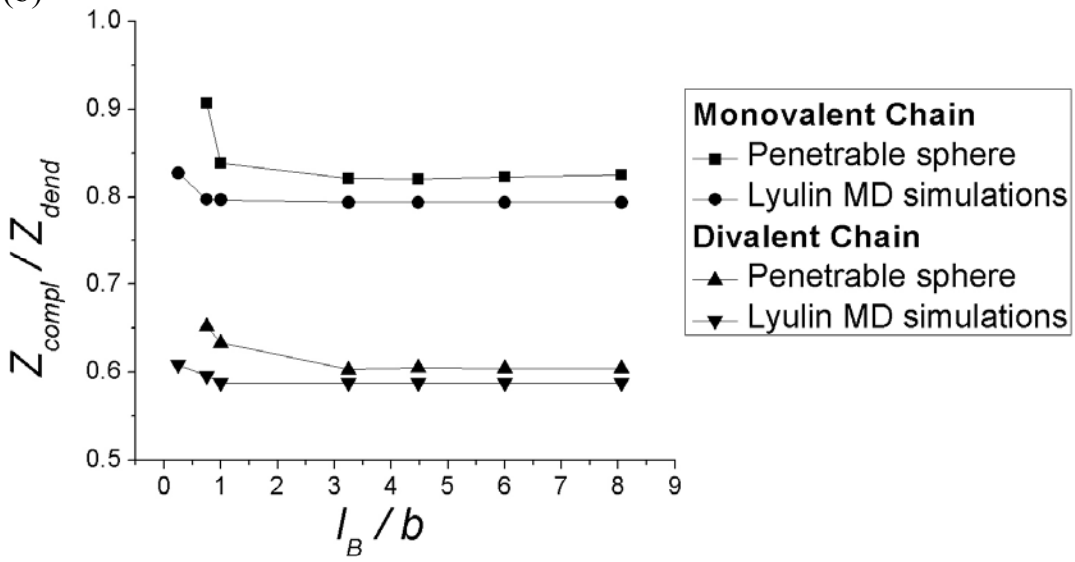

Figure 3.5: (a) The fraction of the chain monomers that condensed on a charged dendrimer of G4 as a function of Bjerrum length l_B and (b) the normalized charge of the complex as a function of the Bjerrum length l_B. The dendrimer modeled as a sphere of radius R = 4nm and charge Z = 48 complexes with an oppositely charged flexible LPE of persistence length l_p=3nm at 1:1 salt concentration corresponds to Debye screening length of 6nm.

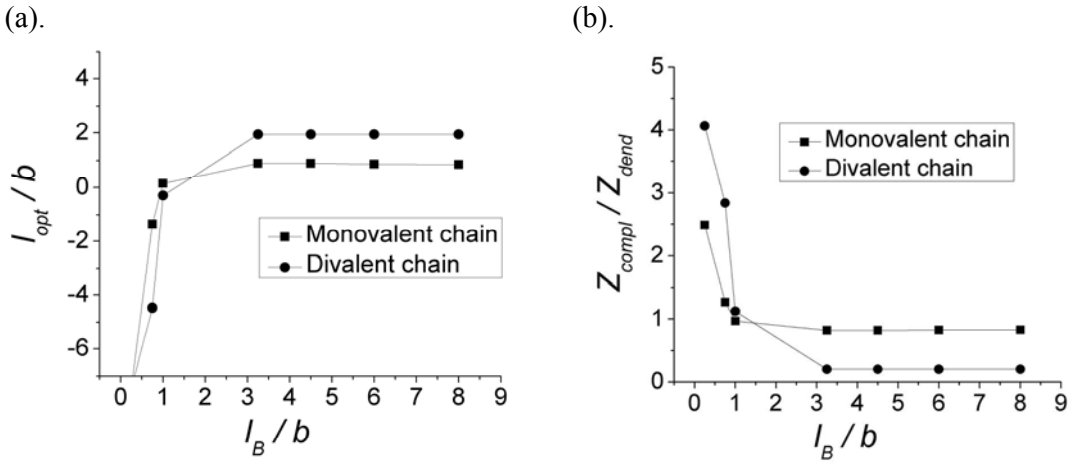

Figure 3.6: The hard sphere model (Schiessel et al., 2001) results for G4-LPE chain complex of (a) The fraction of the chain monomers that condensed on a charged dendrimer of G4 as a function of Bjerrum length l_B and (b) the normalized charge of the complex as a function of the Bjerrum length l_B.

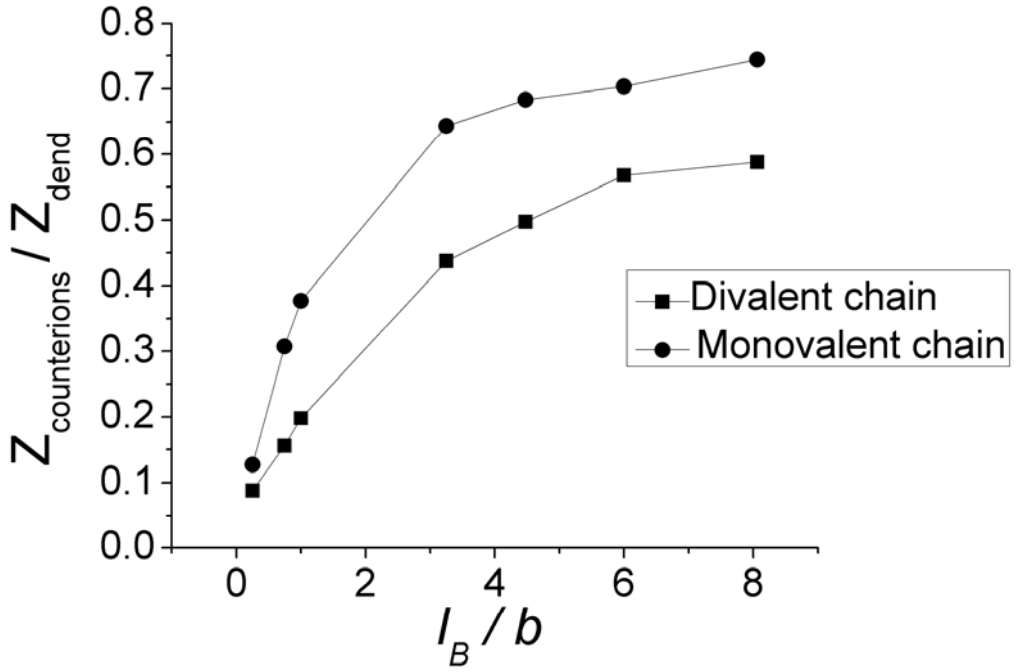

Figure 3.7: Simulation results for $Z_{counterions}/Z_{dendrimer}$ condensed on dendrimer G4-LPE chain complex as a function of Bjerrum length, The dendrimer modeled as a sphere of radius R = 4nm and charge Z = 48 complexes with an oppositely charged flexible LPE of persistence length l_p=3nm at 1:1 salt concentration corresponds to Debye screening length of 6nm (Lyulin et al., 2008)

3.3.2 Effect of LPE chain length on the number of the condensed monomers of chain on PAMAM dendrimer:

The complexation between flexible LPE chain and an oppositely charged sphere has been studied at variant chain lengths L. The sphere modeled as PAMAM dendrimer G3 of charge Z = 24 and R = 3.2nm and LPE chain of persistence length l_p =3nm. Figure 3.8 shows the theoretical prediction of the condensed monomers of LPE on dendrimer by the penetrable sphere model for different lengths of LPE chain to be compared with the predictions of shklovskii hard sphere model (Nguyen and Shklovskii, 2001) and Brownian dynamic simulations (Lyulin, 2005). Upon increasing of the chain length the number of the condensed monomers increase linearly until we reach to chain length which is critical and the number of the condensed monomers at this point is maximum *i.e.*, the overcharging of dendrimer is maximum. We point here that the dendrimer is always overcharged at all chain lengths, all studies are in agreement with each at $L < L_{critical}$, whereas at $L > L_{critical}$, the penetrable sphere model shows a sudden decrease in condensed monomers and then increases again linearly but with a smaller slope, while the hard sphere model shows a saturation in the condensed monomers, finally the BD simulation which shows the maximum overcharging of dendrimer at larger chain length, then at $L > L_{critical}$ the number of the condensed monomers decreases. In general the decrease in the condensed monomers of LPE chain is attributed to the increasing in the electrostatic repulsive free energy between chain monomers which is larger at maximum overcharging of dendrimer.

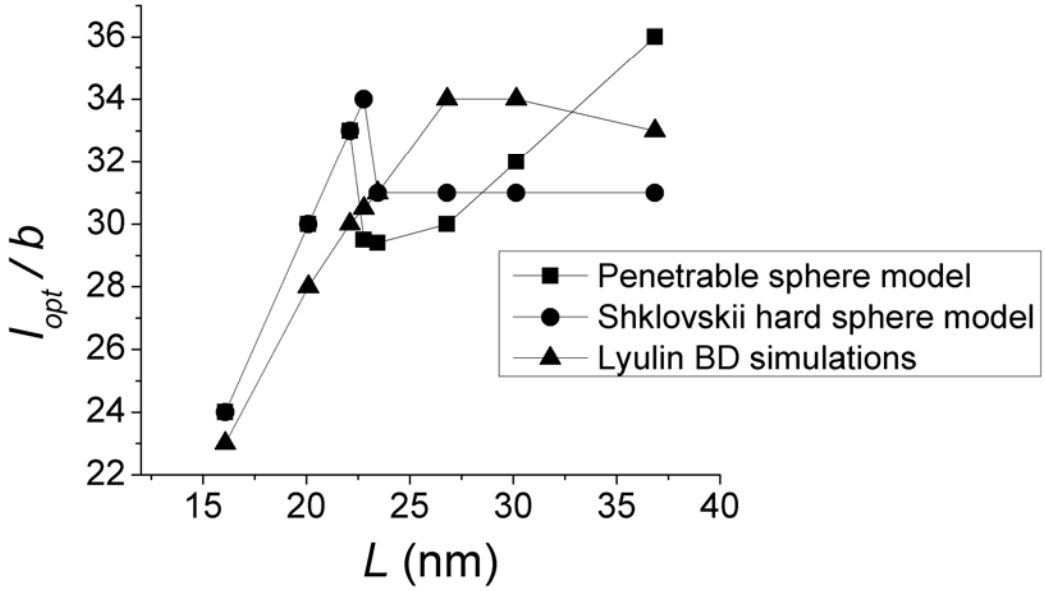

Figure 3.8: The number of the condensed monomers as a function of chain length. The dendrimer modeled as a sphere of radius R = 3.2nm and charge Z = 24 complexes with an oppositely charged flexible LPE of persistence length l_p=3nm at 1:1 salt concentration corresponds to Debye screening length of 6nm.

3.3.3 Effect of salt concentration on PAMAM dendrimer - LPE complex conformation:

For a system of flexible LPE chain of length 33nm and the ammonia cored PAMAM dendrimer G3 of charge Z_{dend} = 24 has been studied for different concentrations of 1:1 salt solution at room temperature which gives 0.71nm of Bjerrum length. From Figure 3.9, upon increasing the concentration of salt the LPE chain become more wrapped around dendrimer where the saturation in the number of the condensed monomers of LPE chain at larger salt concentration is due to the finite and fixed length of the LPE chain. We have two terms in the total free energy equation (Eq. (2.21)) that tend the LPE chain to resist the wrapping around dendrimer namely, the mechanical bending free energy and the electrostatic repulsive free energy between the chain monomers, the latter looses its importance with increasing of salt concentration, these repulsions are balanced by the electrostatic attraction between dendrimer – LPE chain complex, which favors the bending of LPE chain in order to wrap around dendrimer (Kunze and Netz, 2002). The dendrimer is always overcharged, that is, the condensed monomers of the LPE chain on dendrimer exceeds the dendrimer charge, the overcharging degree become larger at higher salt concentration, in other words, when the Debye screening length becomes in order of the spacing between LPE chain monomers, our study is found in agreement with the theoretical studies (Nguyen and Shklovskii, 2001; Boroudjerdi et al., 2011) and computer simulation studies (Luylin et al., 2005; Larin et al., 2009; 2010).

Figures 3.10 shows the total free energy for the PAMAM G3 - LPE complex for two different concentrations of salt solution, $\kappa = 0.1\text{nm}^{-1}$ and $\kappa = 2.5\text{nm}^{-1}$ as a function of wrapping length. The minimized total free energy of the complex was estimated at these concentrations about -16 for $\kappa = 0.1\text{nm}^{-1}$ and -234 for $\kappa = 2.5\text{nm}^{-1}$ each in units of k_BT, this means that the complex conformation at higher salt concentration shows a strong binding interaction in contrast to low salt concentration.

Also the complexation between ethylenediamine cored PAMAM dendrimer of different generations and semiflexible LPE chain of persistence length 50nm has been studied at different concentrations of 1:1 salt solution. The LPE chain modeled DNA molecule of 4331bp equivalents to length of 1472.5nm. Table 3.1 shows the optimal wrapping length of LPE chain around dendrimers of different generations G1, G2, G3, G4, G6 and G8. In Figure 3.11, the fraction of the condensed monomers of LPE chain on dendrimer is displayed. It is shown that for the complex formed by lower generation, namely, G1, G2, G3 and G4 upon increasing of salt concentration the fraction of the condensed monomers on dendrimer increases considerably whereas for higher generations G6 and G8 the fraction of the condensed monomers doesn't change significantly which means that the aggregate formed from the complexation between LPE chain and dendrimer of higher generations seemed to be more neutralized because more and more of DNA charges being get more neutralized by higher generations, this trend is found in agreement with recent experimental study (Carnerup, et al., 2011).

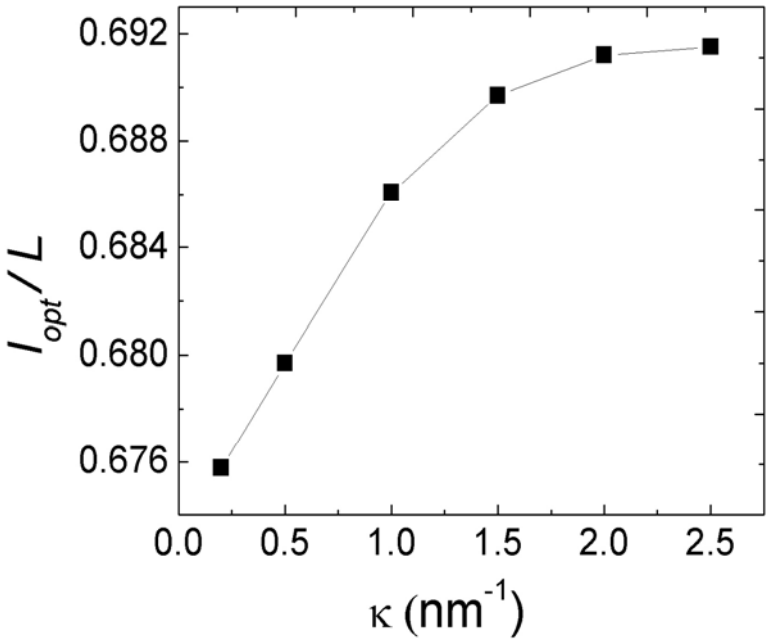

Figure 3.9: The fraction of condensed monomers of LPE chain on ammonia cored PAMAM Dendrimer G3 of charge Z_{dend} = 24 as a function of concentration of 1:1 salt solution, a constant length of flexible LPE equals to L = 33nm corresponds to 47 negatively charged monomers with spacer of 0.7nm, of persistence length equals to 3nm.

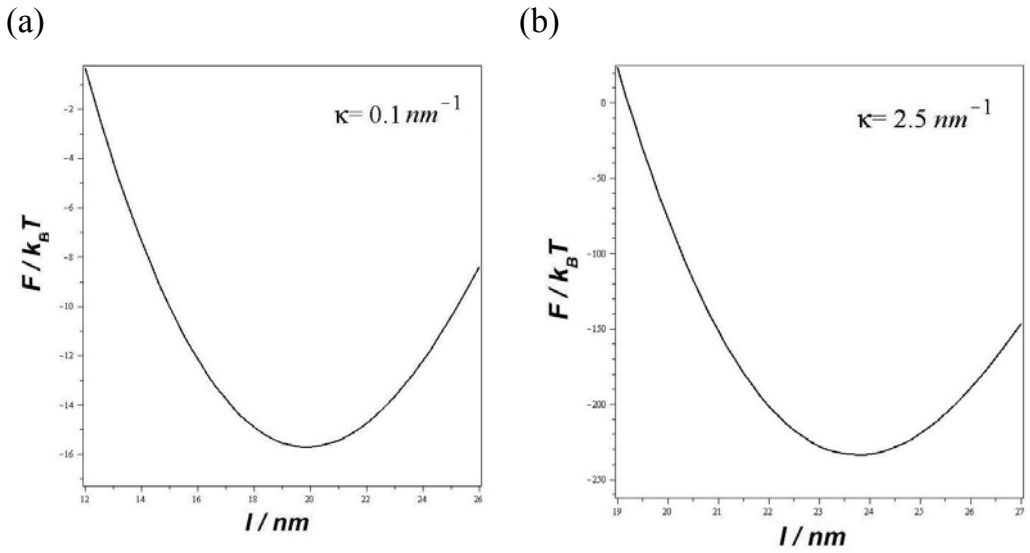

Figure 3.10: The free energy in units of k_BT as a function of the wrapping length at salt concentration (a) for $\boldsymbol{\kappa}$ = 0.1nm^{-1} for and (b) for $\boldsymbol{\kappa}$ = 2.5nm^{-1} for a system of one PAMAM dendrimer of G3 and an appositively charged flexible LPE chain of length L=33nm (47 negatively charged monomers). The dendrimer was considered to be penetrable sphere of radius (R=3.2nm).

Table 3.1: Analytical model results for the interaction between Gx dendrimer and the longer DNA (4331bp), the dendrimer is considered to be a penetrable sphere of radius *R*.

Salt concentration (*mM*)	l_{opt} (*nm*)					
	G1	*G2*	*G3*	*G4*	*G6*	*G8*
10	621	648.52	662.55	673.4	697.61	769.43
30	632.87	656.62	668.29	677.13	698.9	769.49
50	640	661.03	671.19	678.76	699.28	769.37
100	650	666.83	674.64	680.57	699.53	769.17
120	652.43	668.37	675.4	680.88	699.53	769.17
150	655.6	670	676.22	681.19	699.55	769.11
200	660	671.96	677.18	681.6	699.54	769.11

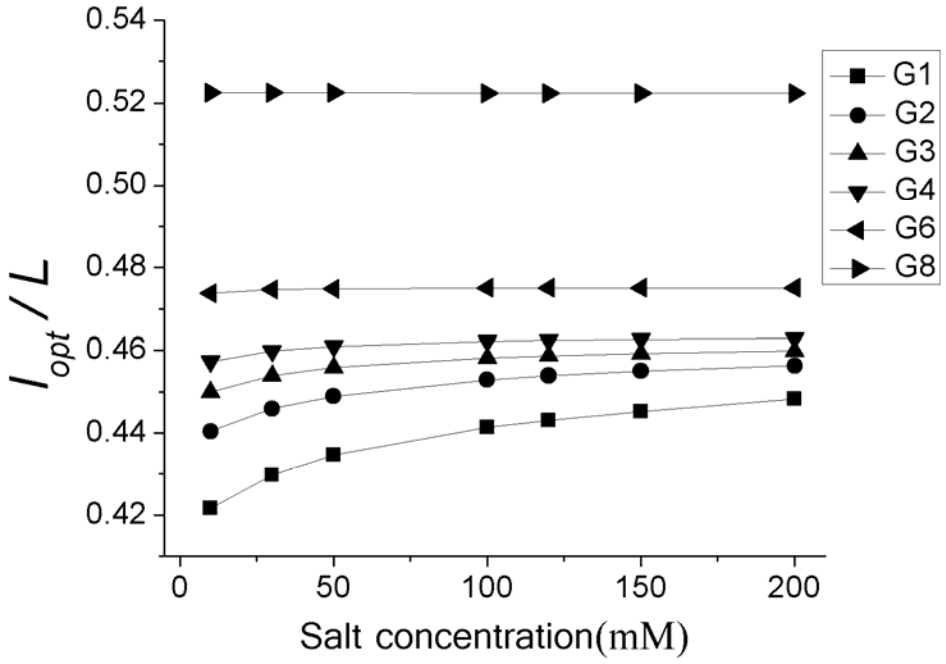

Figure 3.11: The fraction of the condensed monomers of LPE chain as a function of 1:1 salt concentration for a system of one positively charged dendrimer of Gx and an appositively charged semiflexible LPE chain of persistence length l_p = 50nm representing DNA of 4331bp (L=1472.5nm), the dendrimer is considered to be penetrable sphere of radius *R*.

3.3.4 Effect of chain stiffness (Persistence length) on PAMAM dendrimer - LPE complex conformation:

The number of the condensed monomers of the flexible LPE chain on the ammonia cored dendrimer of G4 and the total charge of the complex are studied at different degrees of the chain rigidity. The LPE chain was chosen to bear 16 negatively charged monomers corresponds to a total length of 10.72nm. We pointed here that the length of the chain is much smaller than that is needed to neutralize 48 positively charged monomers on dendrimer of G4, *i.e.*, the overcharging phenomenon of dendrimer will not occur. The rigidity of LPE chain is measured in terms of the persistence length which varied from 3nm to 50nm in the existence of the effect of Bjerrum length, two values of Bjerrum length are considered, l_B= 1.06b represents the complex in the water solution, and l_B=10b represents the complex in the core of the cell membrane.

Figure 3.12a shows the number of the condensed monomers of LPE on dendrimer, it was found that the number of the condensed monomers decreases linearly by increasing of the persistence length of the LPE chain, this trend is found in agreement with the theoretical study that performed by Arcesi and co – workers (Arcesi et al., 2007).

Figure 3.12b shows the total charge of the complex as a function of persistence length, upon increasing of the persistence length of chain as it changes from flexible to rigid, the positive charge of the complex increases considerable especially in the case of l_B=1.04b, since the electrostatic interaction free energy of the complex above certain value of l_p becomes minor relative to mechanical bending free energy of the chain, whereas in the case of l_B=10b the total charge of complex doesn't change significantly because the electrostatic attractive free energy of PAMAM G4 – LPE chain complex is the dominant in this case irrespective of the value of persistence length (chain rigidity). It is expected for larger contour length of LPE chain (*i.e.,* $L >> l_{iso}$), the charge inversion phenomena of the dendrimer well be occurred especially at l_B = 10b and gains its importance which means that the potential ability of LPE chain – dendrimer binding ability to cell membrane become more troublesome since the cell membrane is negatively charged.

We present in Figure 3.13 the total free energy of the LPE chain – dendrimer of G4 complex at different mediums in units of k_BT. Figure 3.13a represents the complex in water phase while the latter represents the complex in the core of the cell membrane, the total free energy was minimized to -0.93, -9.9 each in units of k_BT corresponds to the water phase and the core of cell membrane respectively.

(a)

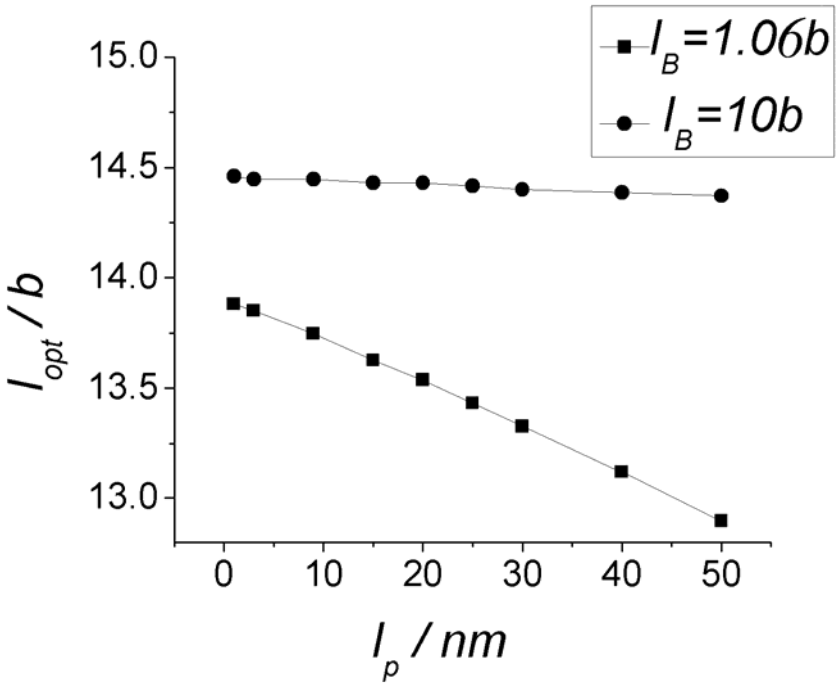

(b)

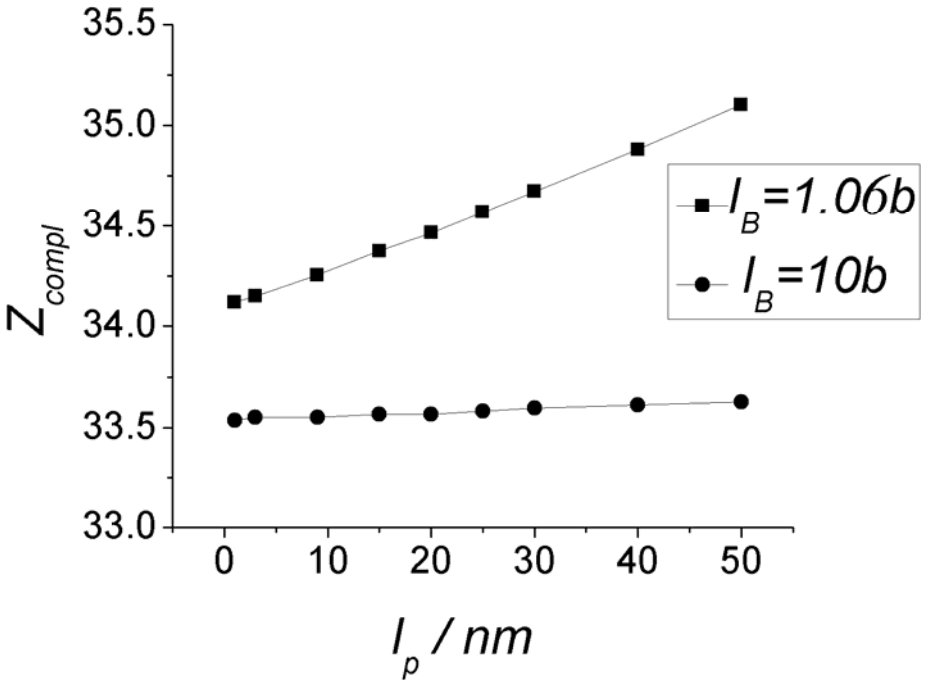

Figure 3.12: The effect of persistence length l_p on (a) the number of the condensed monomers of LPE on dendrimer of G4 and (b) the effective charge of the LPE chain – dendrimer complex, for a system of one dendrimer of G4 of charge Z_{dend} = 48 and an appositively charged flexible LPE of length L=10.72nm equivalent to 16 negatively charged monomer with bond spacer equals to 0.67nm, at 1:1 salt concentration corresponds to 6 nm of Debye length. The dendrimer was considered to be penetrable sphere of radius R=4nm.

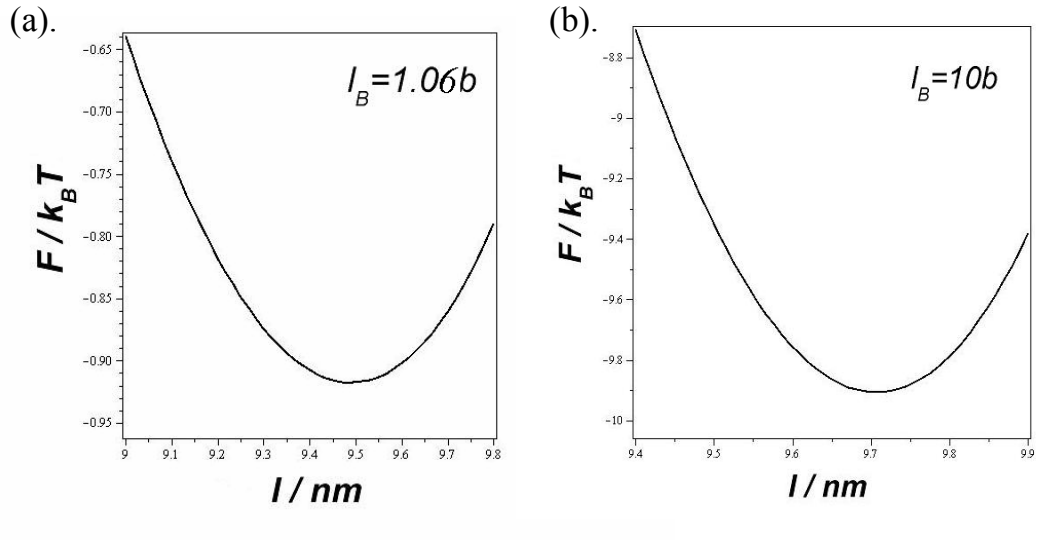

Figure 3.13: Free energy in units of k_BT as a function of the wrapping length (a) in water phase (b) inside cell membrane phase for a system of one dendrimer of G4 of charge Z_{dend} = 48 and an appositively charged flexible LPE of length L=10.72nm equivalent to 16 negatively charged monomers with bond spacer equals to 0.67nm, at 1:1 salt concentration corresponds to 6 nm of Debye length. The dendrimer is considered to be penetrable sphere of radius R=4nm.

The system of DNA and an oppositely single sphere of radius R = 3nm has been studied. According to previous theoretical studies have been used a sphere of different charges Z = 10, 20, and 100, and DNA of 147bp, at 100mM of 1:1 salt solution and 0.71nm of Bjerrum length. The maximum overcharging degree of sphere calculated in terms of $(l_{opt} - l_{iso}) / l_{iso}$ by the penetrable sphere model at zero persistence length. We found that the overcharging degrees are 12.28, 5.91, and 0.82 for charges number 10, 20, and 100 respectively, to be compared with results obtained previously for the hard sphere models by Netz and co-workers (Kunze and Netz, 2002) and Arcesi and co-workers (Arcesi, et al., 2007). As it shown in Table 3.2, the overcharging degree in the case of penetrable sphere shows larger values compared with hard sphere models. This may explained by the difference in values of the total electrostatic interaction free energies of single complex for both penetrable sphere and hard sphere models as it shown in Figure 3.14. In this Figure, the minimized total free energy obtained for penetrable sphere is much larger than that for hard sphere which means that the complexation between DNA and penetrable sphere shows more binding interaction. Also, the complex conformation has been studied at variant values of persistence length for sphere of charge number Z = 20 to be compared to the theoretical prediction by the hard sphere model (Arcesi et al., 2007). Figure 3.15 shows the overcharging degree for both penetrable and hard sphere, upon increasing the persistence length the overcharging degree decreases linearly for both the penetrable sphere and hard models and the overcharging of the penetrable sphere by DNA is always larger than hard sphere which also can be explained by Figure 3.14.

Table 3.2: The overcharging degree of sphere of R = 3nm by DNA of 147bp (L=50nm) at concentration of 1:1 salt solution of 100mM

	Overcharging degree $(l_{opt} - l_{iso}) / l_{iso}$		
Charge number Z	Penetrable sphere model	Hard sphere model (Arcesi et al., 2007)	Hard sphere model (Kunze and Netz, 2002)
10	12.28	7.05	6.23
20	5.91	3.52	3.11
100	0.84	0.71	0.62

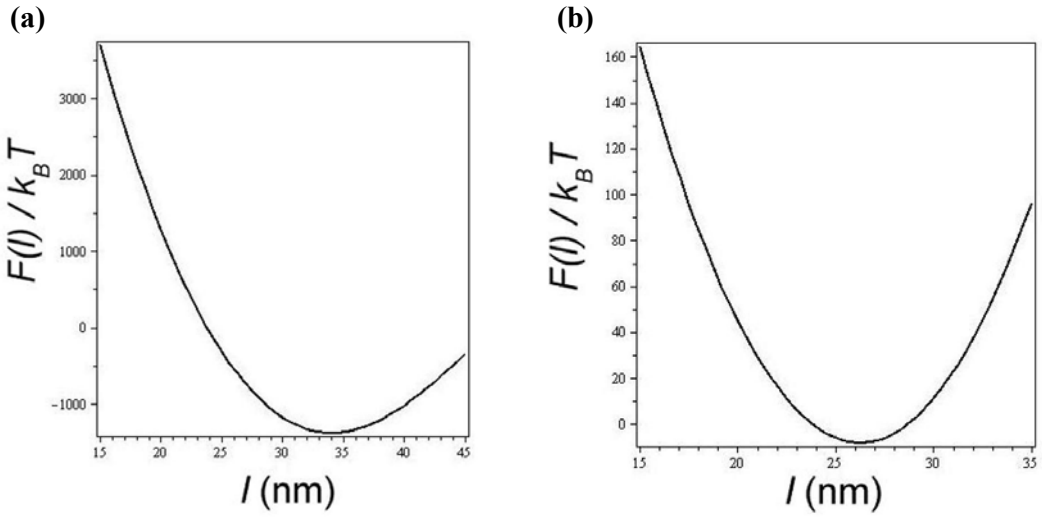

Figure 3.14: Electrostatic interaction free energy in units of k_BT for a system of DNA of 147bp and a single sphere of charge number Z = 100 and radius R = 3nm for (a) penetrable sphere model and (b) hard sphere model

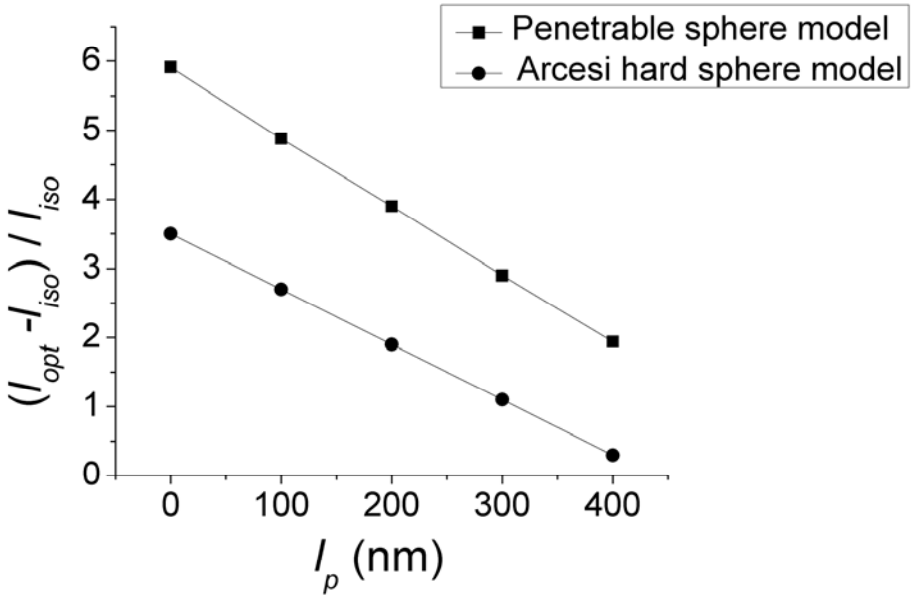

Figure 3.15: Overcharging degree as a function of persistence length. for a system of DNA of 147bp and a single sphere of charge Z = 20 and radius R = 3nm. Salt concentration of 100mM, and Bjerrum length of 0.71nm.

3.3.5 Effect of PAMAM dendrimer charge on the wrapping degree of LPE chain around it:

The charge of histone and other proteins types affects on the wrapping degree of DNA of 147bp around it, the total charge of the complex and the linker formed between two complexes when the charge increases from 50 to 250 are analytically studied by the penetrable sphere model. Figure 3.16a shows the number of turns of LPE chain modeled DNA molecule around protein increases by increasing of the charge of protein until the charge reach above 130, no further increasing in the number of turns of DNA. This behavior is attributed to that the whole 147bp of DNA has been wrapped around protein. As it shown in Table 3.3, the larger wrapping length ranged from 24.23 nm to 24.27nm to give 1.13 to 1.14 turns around each protein, the complexes are very closer to each other with linker takes the range from 0.73nm to 0.77nm. Figure 3.16b shows the total charge of the complex, for small values of charge ($Z < 130$), the complex shows charge reversal which is negative whereas at larger values of the charge ($Z \geq 130$), the net charge of the complex is reversed and increases linearly by increasing of the histone charge.

DNA wrapping around different proteins in terms of number of turns has been experimentally (Richmond and Davey, 2003) and theoretically (Arcesi et al., 2007) investigated. We can apply the penetrable sphere model to determine the wrapping length of DNA molecule of 147bp of persistence length l_p = 50nm around an octamer or other types of proteins represented by PAMAM dendrimer of different charges Z at physiological conditions, and at salt concentration of 100mM of 1:1 salt solution which corresponds to 0.96nm of Debye screening length and at 0.71 of Bjerrum length.

Table 3.4 represents the theoretical predictions of DNA wrapping degree around proteins by our theoretical study and previous theoretical study (Arcesi et al., 2007). Besides the experimental data obtained from X-ray and electron–microscopy (Richmond and Davey, 2003) are shown. the 147bp of DNA wrap around an octamers of charges number Z = 100 and 134 each of radius R = 3.4nm gave the number of turns to be 1.43 and 1.59 respectively by our model. While Arcesi and co – workers showed 1.08 and 1.29. The experimental results take the range from 1.58 – 1.59 turns. For a protein of charge number Z = 14 and radius R = 4nm, our model showed the number of turns equals to 0.87, while Arcesi and co – workers showed 0.60. Furthermore the experimental result was 0.95. It was found that the results obtained by the penetrable sphere model are much closer to the experimental results compared to the results obtained previously by theoretical study (Arcesi et al., 2007).

Table 3.3: Analytical model results for the interaction between two dendrimer – DNA complexes with a linker D' between their surfaces, dendrimers are considered a penetrable sphere with radius R = 3.4nm carries different charges number Z_{dend}, and highly charged PE representing DNA consists of 147bp.

Charge number Z_{dend}	$l_{opt}(nm)$	Z_{compl}	$D'(nm)$	*No. of Turns*
50	15.28	-39.88	9.72	0.72
100	20.26	-19.18	4.74	0.95
130	24.27	-10.58	0.73	1.14
150	24.27	7.23	0.73	1.14
200	24.27	57.23	0.73	1.14
250	24.23	107.47	0.77	1.13

Table 3.4: The number of DNA turns around octamer and other CSB proteins determined by penetrable sphere model, previous theoretical model and resulting from x-ray and electron-microscopy experiments for DNA of 147bp and 100mM of 1:1 salt solution.

		Present Theoretical study (penetrable sphere)		Previous Theoretical Study (hard sphere) (Arcesi et al., 2007)		Experimental Results (Richmond and Davey, 2003)
R (*nm*)	*Charge number Z*	L_{opt} (*nm*)	*No. of Turns*	L_{opt} (*nm*)	*No. of Turns*	*No. of Turns*
3.4	100	30.55	1.43	23.06	1.08	1.58 – 1.59
3.4	134	33.86	1.59	27.54	1.29	
4	14	21.96	0.87	15.07	0.60	0.95

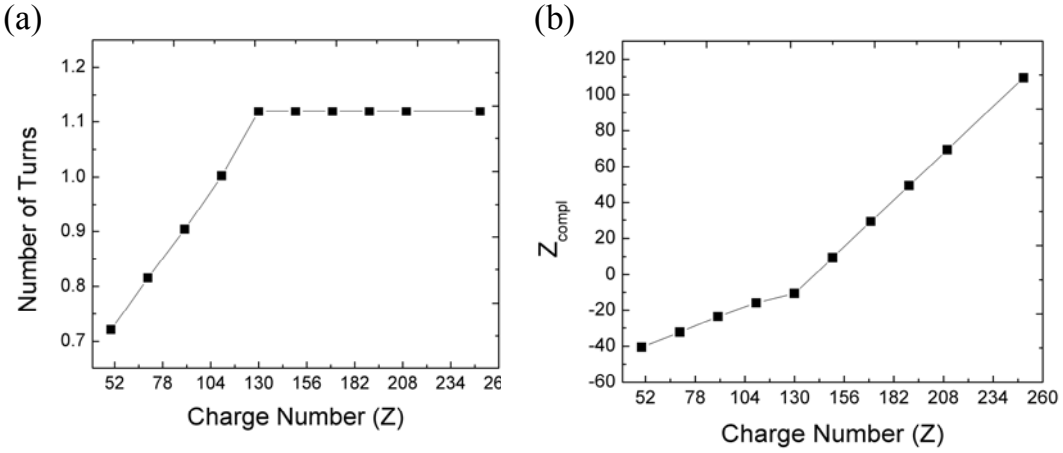

Figure 3.16: Effect of dendrimer charge on (a) the number of turns on the dendrimer and (b) the total charge of the complex for a system of two positively charged dendrimers each of charge Z_{dend} and an appositively charged semiflexible LPE of length $L \approx$ 50nm representing DNA of 147bp, the dendrimers are considered penetrable spheres of R=3.4nm.

3.4 System of a multiple PAMAM dendrimers – LPE chain complexes

3.4.1 Effect of PAMAM dendrimer contraction on the structural properties of dendrimers – LPE aggregate:

In addition to the fact that dendrimers are considered to be ion-penetrable charged spherical particles (porous sphere) as it assumed in this study, they are also proved to have a soft structure of high flexibility (Rosenfeldt et al., 2002; Likos et al., 2002). Their internal structure and size are controlled by the intermolecular electrostatic repulsion. When dendrimer interact with an oppositely charged DNA they are likely to contract in smaller size. That is the reduction of the size of dendrimer as the radius changes from $R=R_0$ to $R=0.4R_0$ will be taken into account in accordance to Qamhieh and co-workers study (Qamhieh et al., 2009) to exceed the experimental observations (Dootz et al., 2011).

The aggregate formed between PAMAM dendrimer – DNA complexes has been studied. The charge of dendrimer of different generations G2, G4, G6 and G8 at neutral pH are: 16, 64, 256 and 1024, respectively. Semi-flexible rod of persistence length l_p = 50nm is used to represent DNA molecule of 2000bp and 4331bp. According to experimental study, the fluorescence spectroscopy results for the interaction between dendrimer – DNA aggregate for different generation are summarized in Table 3.5.

Tables 3.6 – 3.10 show the effect of the reduction of the dendrimer size on the optimal wrapping length of DNA around dendrimer, total charge of the dendrimer – DNA aggregate, and other structural properties of the aggregates. The concentration of 1:1 salt solution 10mM of NaBr which corresponds to 3nm of the Debye screening length and 0.71nm of Bjerrum length at room temperature. The dendrimers are considered to be a penetrable spheres with dendrimer-dendrimer spacing $D(N,l)=(L-Nl+2NR)/N$.

Table 3.5: The number of dendrimers bound per DNA molecule and the charge ratio of the dendrimer – DNA complex as estimated from experimental data in dilute aqueous solutions

Dendrimer	G2	G4	G6	G8
N_{exp}	318	140	16	5
$r_{charge}=N_{exp}Z_{dend}/Z_{chain}$	0.58	1.03	0.47	0.59

Table 3.6: Analytical model results for the interaction between G2 dendrimers and the DNA (4331 bps), N = 318 and L = 1472.5 nm, Z_{dend} =16.

x (R=xR_o)	l_{opt} (nm)	*Diff* (nm)	Z^*_{compl}	Z^*_{compl}/Z	$D(N,l)$ (nm)	$D'(N,l)$ (nm)	$(D'+diff)N/L$	*Ratio* $l_{opt}/2\pi R$	F_{int}/F_{min}	$F_{bending}$ (k_BT)
1.00	3.59	0.87	-5.117	-0.319	3.94	1.04	0.412	0.39	0.0001	13574.5
0.90	3.59	0.87	-5.117	-0.319	3.65	1.04	0.412	0.44	0.0002	16758.7
0.80	3.59	0.87	-5.117	-0.319	3.36	1.04	0.412	0.49	0.0003	21210
0.70	3.58	0.86	-5.058	-0.316	3.08	1.05	0.412	0.56	0.0003	27626
0.60	3.58	0.86	-5.058	-0.316	2.79	1.05	0.412	0.66	0.0004	37602
0.50	3.58	0.86	-5.058	-0.316	2.50	1.05	0.412	0.79	0.0005	54146.9
0.40	3.58	0.86	-5.058	-0.316	2.21	1.05	0.412	0.98	0.0006	84604.6

Table 3.7: Analytical model results for the interaction between G4 dendrimers and the DNA (4331bps), N = 140 and L = 1472.5 nm, Z_{dend} = 64.

x (R=xR_o)	l_{opt} (nm)	*Diff* (nm)	Z^*_{compl}	Z^*_{compl}/Z	$D(N,l)$ (nm)	$D'(N,l)$ (nm)	$(D'+diff)(N)/L$	*Ratio* $l_{opt}/2\pi R$	F_{int}/F_{min}	$F_{bending}$ (k_BT)
1.00	10.51	-0.37	2.176	0.03	4.50	0.00	-0.03	0.74	0.0012	7266.2
0.90	10.51	-0.37	2.176	0.03	4.05	0.00	-0.03	0.83	0.0012	8970.6
0.80	10.51	-0.37	2.176	0.03	3.67	0.00	-0.03	0.93	0.0013	11353.4
0.70	10.51	-0.37	2.176	0.03	3.15	0.00	-0.03	1.06	0.0013	14828.9
0.60	10.51	-0.37	2.176	0.03	2.71	0.00	-0.03	1.23	0.0013	20183.8
0.50	10.51	-0.37	2.176	0.03	2.26	0.00	-0.03	1.48	0.0012	29064.7
0.40	10.51	-0.37	2.176	0.03	1.81	0.00	-0.03	1.85	0.0011	45413.6

Table 3.8: Analytical model results for the interaction between G6 dendrimers and the DNA (4331bps), N = 16 and L = 1472.5 nm, Z_{dend} = 256.

(R=xR_o)	l_{opt} (nm)	*Diff* (nm)	Z^*_{compl}	Z^*_{compl}/Z	$D(N,l)$ (nm)	$D'(N,l)$ (nm)	$(D'+diff)(N)/L$	*Ratio* $l_{opt}/2\pi R$	F_{int}/F_{min}	$F_{bending}$ (k_BT)
1.00	65.63	22.1	-130	-0.50	33.1	26.4	0.52	3.11	1.3E-8	2339.2
0.90	65.63	22.1	-130	-0.50	32.43	26.4	0.52	3.40	1.7E-8	2887.9
0.80	65.63	22.1	-130	-0.50	31.76	26.4	0.52	3.89	2.1E-8	5655.0
0.70	65.62	22.1	-130	-0.50	31.1	26.4	0.52	4.45	2.7E-8	4773.2
0.60	65.62	22.1	-130	-0.50	30.43	26.4	0.52	5.19	3.4E-8	6496.8
0.50	65.60	22.08	-129.9	-0.50	29.78	26.4	0.52	6.23	4.3E-8	9352.6
0.40	65.57	22.05	-129.7	-0.50	29.14	26.4	0.52	7.79	5.4E-8	14606.8

Table 3.9: Analytical model results for the interaction between G8 dendrimers and the DNA (4331bps), N = 5 and L = 1472.5 nm, Z_{dend} = 1024.

x (R=xR_o)	l_{opt} (nm)	*Diff* (nm)	Z^*_{compl}	Z^*_{compl}/Z	$D(N,l)$ (nm)	$D'(N,l)$ (nm)	$(D'+diff)(N)/L$	*Ratio* $l_{opt}/2\pi R$	F_{int}/F_{min}	$F_{bending}$ (k_BT)
1.00	228.7	54.62	-321.29	-0.31	75.5	65.8	0.408	7.50	9E-15	1215.3
0.90	228.71	54.63	-321.3	-0.31	74.5	65.7	0.408	8.34	1.2E-14	1500.5
0.80	228.71	54.63	-321.35	-0.31	73.5	65.79	0.408	9.38	1.6E-14	1899.0
0.70	228.70	54.62	-321.29	-0.31	72.59	65.8	0.408	10.72	2.2E-14	2480.3
0.60	228.68	54.60	-321.17	-0.31	71.64	65.8	0.408	12.51	2.8E-14	3375.6
0.50	228.63	54.55	-320.88	-0.31	70.72	65.87	0.408	15.00	4E-14	4859.8
0.40	228.53	54.45	-320.29	-0.31	69.85	65.97	0.408	18.75	5.4E-14	7590.1

Table 3.10: Analytical model results for the interaction between G4 dendrimers and the DNA (2000bps), N = 35 and L = 680 nm, Z_{dend} = 64.

x (R=xR_o)	l_{opt} (nm)	*Diff* (nm)	Z^*_{compl}	Z^*_{compl}/Z	$D(N,l)$ (nm)	$D'(N,l)$ (nm)	$(D'+diff)(N)/L$	*Ratio* $l_{opt}/2\pi R$	F_{int}/F_{min}	$F_{bending}$ (k_BT)
1.00	14.72	3.84	-22.58	-0.35	9.2	4.7	0.44	1.04	0.0001	2544.2
0.90	14.72	3.84	-22.58	-0.35	8.76	4.7	0.44	1.15	0.0001	3140.9
0.80	14.72	3.84	-22.58	-0.35	8.3	4.7	0.44	1.30	0.0001	3975.3
0.70	14.72	3.84	-22.58	-0.35	7.85	4.7	0.44	1.48	0.0002	5192.2
0.60	14.71	3.83	-22.52	-0.35	7.42	4.7	0.44	1.73	0.0002	7062.4
0.5	14.70	3.82	-22.47	-0.35	6.97	4.7	0.44	2.00	0.0003	10162.9
0.40	14.68	3.80	-22.35	-0.35	6.54	4.7	0.44	2.59	0.0004	15858.0

From Table 3.6 the optimal wrapping length of DNA around ethylenediamine cored PAMAM dendrimer of G2 doesn't change significantly when dendrimer radius is decreased. As a result the difference between the optimal wrapping length and the isoelectric length ($Diff = l_{opt} - l_{iso}$) is slightly constant. The net charge of the nucleosome of G2 Dendrimer – DNA complex remains roughly constant and always negative when dendrimer shrink upon the interaction with an oppositely charged LPE chain. This means that the charge of dendrimer is inverted, the absolute value of the charge inversion ratio of the G2 – DNA nucleosome $|Z_{compl}(l)/Z_{dend}|\times 100\%$ of order ~ 32%. The G2 dendrimer – DNA aggregate has a slightly total fixed charge of order ~ -1590e. Also the center-to-center spacing between complexes $D(N,l)$ was shown to decrease from 3.94 to 2.21nm when R reduced from R_0 to $0.4R_0$. This illustrates the slightly increasing in the ratio of the electrostatic repulsion free energy between complexes to the total minimized free energy of aggregate. Nevertheless, the linker between complexes ($D' = D - 2R$) doesn't affected by the reduction of the size of the dendrimer. It has a constant value and equals to 1.05nm which means that the surface contact between two complexes are kept at fixed separation irrespective how much the dendrimer contracts. The ratio between the optimal wrapping length (l_{opt}) and the circumference of complex was found to increase from 0.39 to 0.98 when dendrimer R is decreased. The ratio between the un-neutralized length of DNA and the contour length of DNA is constant and equals to 0.41 which gives the neutralized part of the DNA of order 59%. The bending free energy of the DNA increases rapidly with decreasing radius R. The smaller size and charge of dendrimer of G2 illustrates the smaller ratio between l_{opt} and the circumference of the complex among all generations.

Whereas in G4 dendrimer – DNA aggregate, the optimal wrapping length around G4 dendrimer is constant which equals to 10.51nm as shown in Table 3.7. The difference between the optimal length and the isoelectric length has a constant value -0.37nm. The negative sign indicates that dendrimer of G4 is not completely neutralized by oppositely charged DNA molecule. This gives a slightly positive charge of the nucleosome formed by G4 dendrimer – DNA complex which equals to +2.176. The dendrimer G4 – DNA

aggregate has a total positive charge of +304.6*e*. In this case the charge of the DNA is inverted completely by G4 dendrimer. As well as the neutralized part of DNA is ~100%. These results reveal the importance of the charge inversion in gene delivery since the cell membrane is negatively charged. The center-to-center separation between G4 dendrimer – DNA complexes is reduced from 4.50 to 1.81nm when dendrimer radius R is decreased, with zero linker between G4 dendrimer – DNA complexes. Upon the contraction of the dendrimer the ratio between the repulsive electrostatic interaction and the total minimized free energy is slightly constant.

Table 3.8 shows the optimal length that wrapped around dendrimer of G6 doesn't change significantly when the dendrimer contracts. The difference between l_{opt} and l_{iso} shows a slightly fixed value of order ~22.1nm. The net charge of the nucleosome of G6 dendrimer – DNA complexes is slightly constant in order -130 whatever dendrimer shows contraction, and for G6 Dendrimer – DNA aggregate to have a total negative charge of -2080*e.* The absolute value of the charge inversion ratio of the G6 – DNA nucleosome of order ~ 50%. The center-to-center separation between G6 dendrimer – DNA complexes was shown to decrease from 33.1 to 29.14. The linker was shown to be constant with value of 26.4nm. The non-neutralized part of DNA is 0.52 which gives 48% of the neutralized part of DNA by G6 dendrimer in the aggregate. The ratio between the repulsive electrostatic interaction between complexes and the minimized total free energy and the mechanical bending free energy of G6 dendrimer – DNA complex are found to increase when the radius of the dendrimer reduced. From Table 3.8, the optimal length that wrapped around dendrimer of G6 doesn't change significantly when the dendrimer contracts. The net charge of the nucleosome of G6 dendrimer – DNA complexes is also slightly constant in order -130 whatever dendrimer shows contraction where the G6 Dendrimer – DNA aggregate has a total negative charge of -2080*e.* The absolute value of the charge inversion ratio of the G6 – DNA nucleosome ~ 50%. The center-to-center separation between G6 dendrimer – DNA complexes was shown to decrease from 33.1 to 29.14 with a linker with constant value of 26.4nm. The non-neutralized part of DNA is 0.52 gives 48% of the neutralized part of DNA by G6 dendrimer in the aggregate. For higher generations such as G8 as it shown in Table 3.9, as the radius of dendrimer decreased, the aggregate of G8 – DNA complexes have the smallest bending free energy. In this case, the smallest ratio between the electrostatic repulsive free energy between complexes and minimized total free energy of the aggregate. The optimal wrapping length of DNA around dendrimer of G8 was found to have a slightly fixed value of order ~ 228.7nm when the dendrimer contracts by the complexation with LPE chain. The center-to-center spacing between G8 dendrimer – DNA complexes is the largest with comparison with lower generations which takes the range from 75.5 to 69.85nm as R decreased from R_0 to $0.4R_0$. The linker formed between G8 dendrimer – DNA complexes has a slightly fixed value of 65.8nm. The aggregate of G8 – DNA complexes has a slightly constant negative total charge of -1600e, while the absolute value of the charge inversion ratio of the G8 – DNA nucleosome about ~ 31%.

The complexation between DNA molecules and dendrimer of G4 is also investigated for shorter contour length of 680nm corresponding to 2000bp of DNA. Nevertheless, we did not see any discrepancy in what obtained earlier for the complexation of dendrimer of different generations with DNA of length 4331bp. As it can be seen from Table 3.10, the optimal wrapping length of DNA around dendrimer of G4 of order ~14.7nm when dendrimer contracts. The absolute value of the charge inversion ratio of the nucleosome is

of order ~35%, while dendrimer – DNA aggregate has a slightly constant and negative charge of -799.4*e*. The neutralized part of DNA is about 56%.

To summarize the results obtained by the penetrable sphere model for the interaction between DNA molecule and dendrimer of different generations as presented in Tables 3.6 – 3.10. A comparison between the obtained results and other obtained results are made (Qamhieh et al., 2009; Qamhieh et al., in progress). In our study, we found that the optimal wrapping length doesn't change significantly irrespective of dendrimer contracts or not. On the contrary Qamhieh and co – worker in their study showed that the optimal wrapping length decreases by decreasing the dendriemr radius. Also we have showed that the net charge of the complexes for all generation doesn't change significantly upon the contraction while Qamhieh and co – workers showed that the net charge of complexes for lower generations G2 and G4 changes from negative to positive when dendrimer radius deceased while for higher generation the net charge is negative. We showed that the linker between complexes for all generation doesn't change when dendrimer contracted in contrast to the other study which showed that the linker increases with the decrease of dendrimer radius. The number of turns of DNA around dendrimer increased for all generations when the radius of the dendrimer is decreased, while Qamhieh and co – workers showed that the number of turns were found to decrease when dendrimer radius is decreased for G2. For higher generation the number of turns obtained by Qamhieh and co – workers are in accordance to what obtained by our study.

Figure 3.17 shows the effect of dendrimer generation on the optimal wrapping length of DNA. The difference between the optimal wrapping length and the isoelectric length (*Diff*) around dindrimer of different generations G2, G4, G6, and G8, is as follows: Upon increasing of generation both l_{opt} and (*Diff*) are increasing with non-linear relation. This large growth may attributed the fact that the number of functional primary amine groups (*Z*) increases exponentially with generations. A schematic representation reveals the effect of generation on the number of turns of DNA around dendrimer and takes into account the reduction in the dendrimer radius due to complexation with DNA according to experimental study (Dootz et al., 2011) as it shown in Table 3.11. The total free energy for a system of DNA – dendrimer aggregates for different generations G2, G4, G6 and G8 and DNA molecule of 2000bp and 4331bp. According to the experimental results obtained previously (see Table 3.5), the minimized total free energies in units of k_BT are plotted as a function of wrapping length as shown in Figures 3.18a – 3.18d. The estimated free energies at the optimal wrapping length (l_{opt}) for the aggregates of 4331bp of DNA – dendrimer of generation G2, G4, G6 and G8 are as follows: -7.82×10^5, 8537, -1.62×10^6 and -1.1×10^6 respectively, and the aggregate of 2000bp of DNA – dendrimer of G4 the estimated total free energy is -1.75×10^5 see Figure 3.18e.

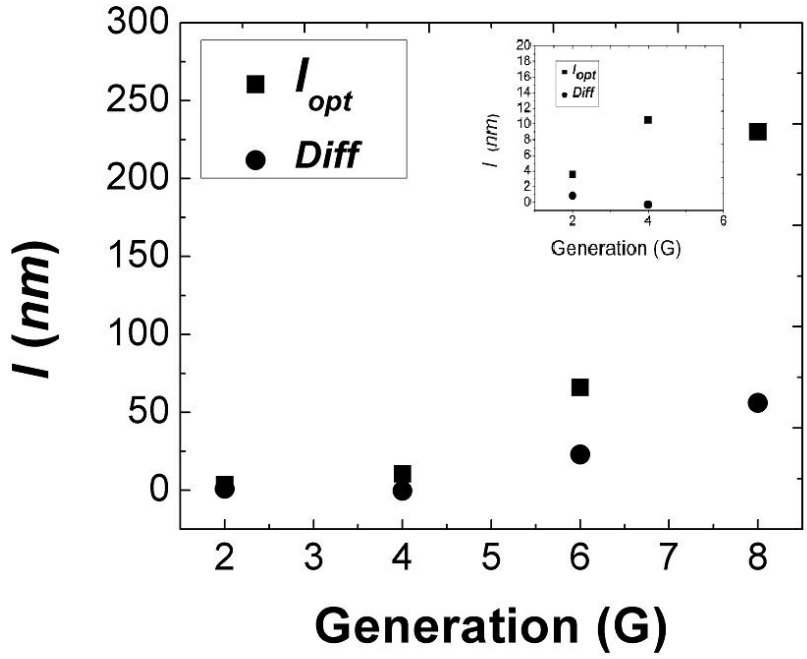

Figure 3.17: The optimal wrapping length and the difference between the optimal wrapping length and the isoelectric length (*Diff*) as a function of generation for 1472.5nm (4331bps) of semiflexible DNA chain of persistent length l_p = 50nm with an axial spacing between phosphate groups b=0.17nm.

Table 3.11: Schematic representation shows the effect of PAMAM dendrimer generations (size and charge) on the number of turns of DNA around dendrimer.

Complex	*G2-DNA*	*G4-DNA*	*G6-DNA*	*G8-DNA*
$R=0.9R_0$ (nm)	*1.31*	*2.03*	*3.02*	*4.37*
Schematic Representation				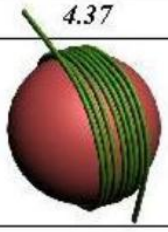
Number of turns	*0.4*	*0.8*	*3.4*	*8*

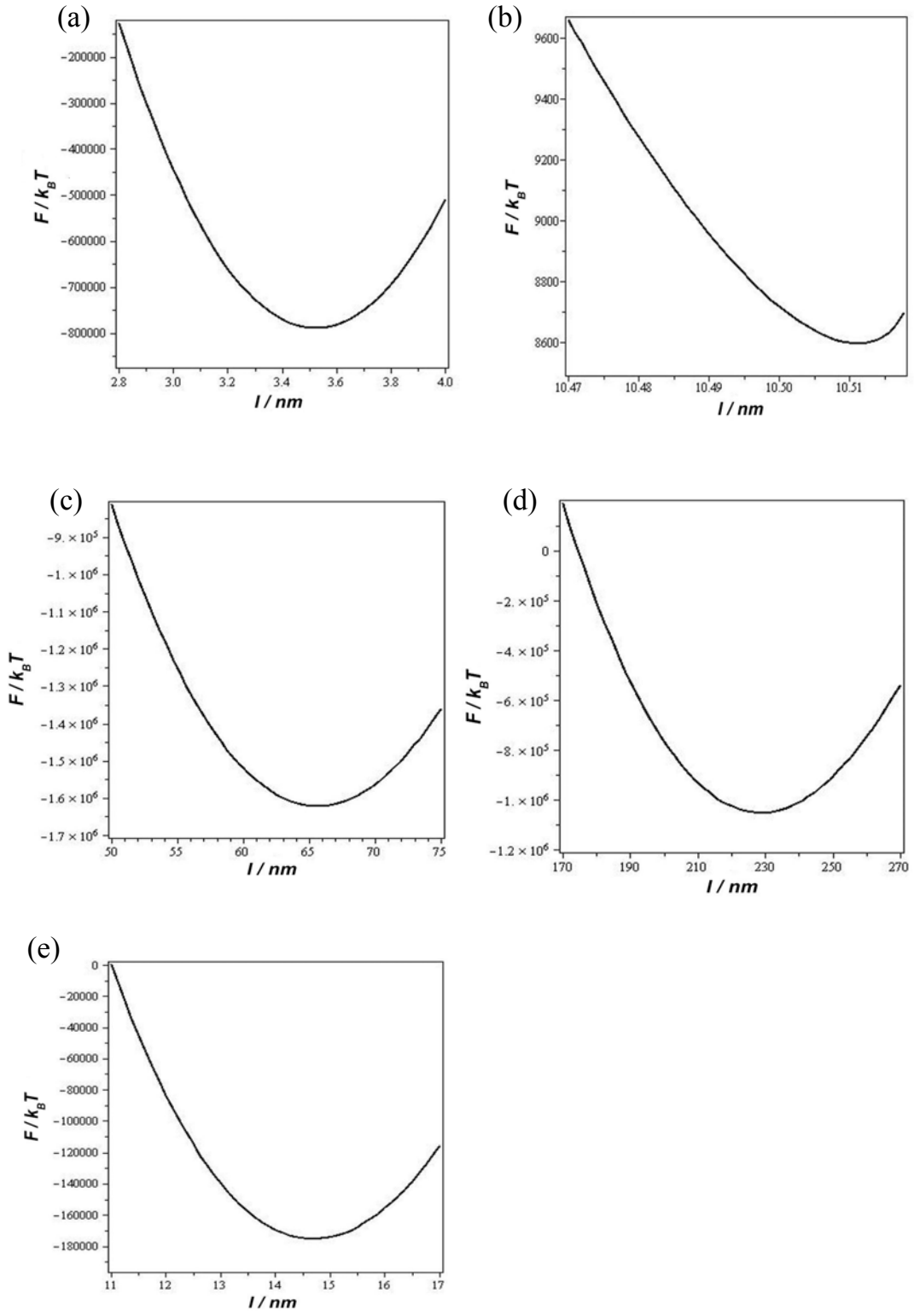

Figure 3.18: The total free energy in units of k_BT as a function of the wrapping length for a system of (a) G2/ DNA of 4331bp aggregate, (b) G4/DNA of 4331bp aggregate, (c) G6/DNA of 4331bp aggregate, (d) G8/ DNA of 4331bp aggregate , (e) G4/ DNA of 2000bp aggregate. The dendrimers are considered to be penetrable sphere of radius *R*.

3.4.2 Linker formation between complexes:

The effect of the Bjerrum length, pH value and the length of the LPE chain on the linker formed between 2Gx – LPE chain complexes have been studied.

The total free energy was minimized in order to get stable LPE chain – 2G3 complexes for different LPE lengths. In all cases the LPE exceeds the length needed to neutralize the 2G3 dendrimer. As it shown in Figure 3.19, the configuration of the complexes strongly depends on the length of the LPE chain. The total length of LPE divided into two parts, the optimal wrapping length and the linker. The optimal wrapping length increases with increasing LPE length until it reach to the critical value of the chain length. Above this critical length, the linker appears and then decreases with the increasing of chain length. Comparing with the result by BD simulations (Larin et al., 2010), which shows smaller linker formation, this linker is shown to increase slowly with the increasing of the chain length. Schematic representation shows the effect of chain length on the linker and the optimal wrapping length obtained by the penetrable sphere model is shown in Figure 3.19.

For a complexation of dendrimers of G3 with flexible LPE chain when it moves from the water phase through the membrane - water interface to the core of the membrane. Figure 3.20 shows the effect of the Bjerrum length on the linker formed between LPE chain – 2G3 complexes. As it shown when the ratio of l_B / b increases, *i.e.,* when the attractive electrostatic interactions increase, the optimal wrapping length increases as a result the linker decreases significantly. We attribute the reduction of the linker between complexes to the increasing of the number of condensed monomers of the chain on the dendrimer. As well as the reduction of positive charge of the complex, as a result the repulsive electrostatic interaction between complexes decreases.

We present in Figure 3.21 the effect of pH value on the linker formed between 2G6 – LPE complexes and the optimal wrapping length of LPE chain around PAMAM dendrimer of G6. In more acidic conditions, we have the largest wrapping length of LPE chain around dendrimer, as a result the linker formed between complexes is small.

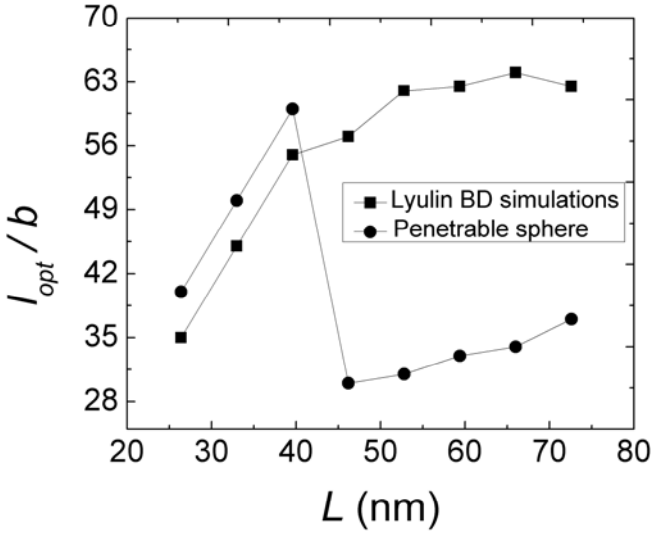

Figure 3.19: The number of the condensed monomer of the chain on dendrimer a function of chain length. A system of 2G3 complexes with an oppositely charged flexible LPE of persistence length of 3nm and monomers spacer of 0.7nm. 100nm of Debye screening length.

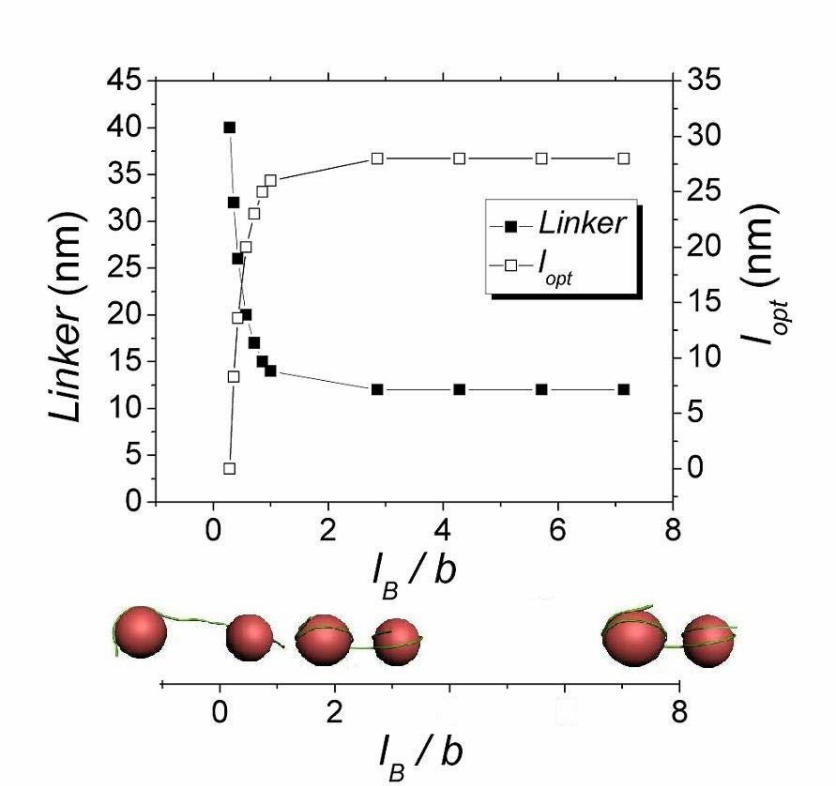

Figure 3.20: Linker formed between 2G3 complexes with an oppositely charged flexible LPE as a function of Bjerrum length. The LPE chain has persistence length of 3nm and monomers spacer of 0.7nm of a contour length of the flexible LPE of length 80nm, the dendrimers are considered as a penetrable spheres with radius R = 3.2nm.

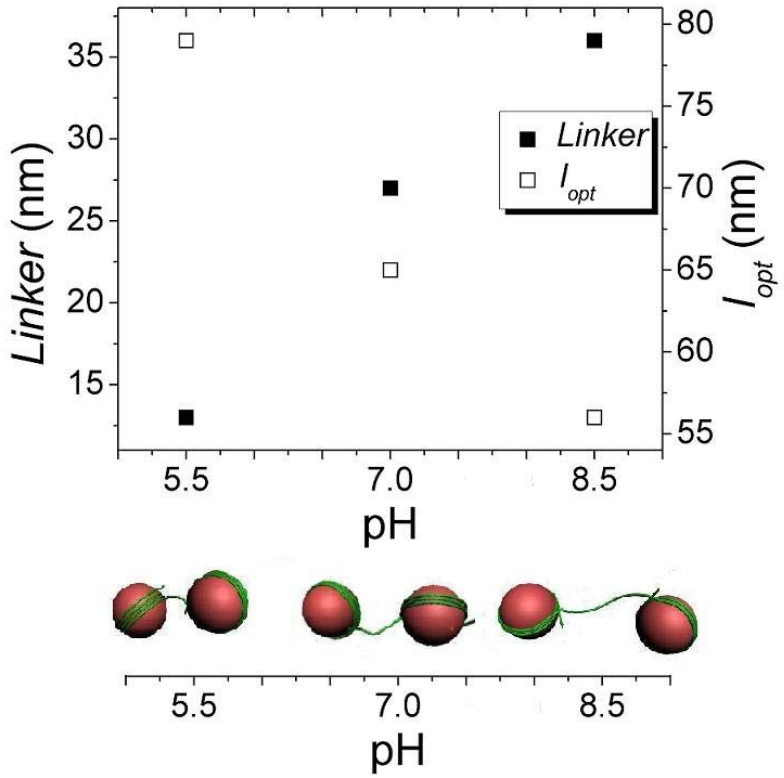

Figure 3.21: Linker formed between 2G6 – DNA complexes as a function of pH value. The LPE chain modeled DNA molecules of 541bp (184nm), the dendrimers are considered as a penetrable spheres with radius R = 3.5nm.

Chapter Four

Conclusion and Future Work

Chapter Four

Conclusion and Future Work

The analytical study presented here is the first theoretical study of the complexation between LPE chain and a penetrable sphere. Throughout this study we concentrated on the effect of the medium's environments on the complex conformation, namely, the concentration of salt for the case of 1:1 salt solution, dielectric permittivity of the solvent, pH conditions and other factors such as the effect of the dendrimer generation (size and charge). The degree of polymerization of the LPE chain and also the rigidity of the LPE chain. We found that the wrapping degree of LPE chain around dendrimer and the binding affinity of the complex formed between LPE chain and a single dendrimer increases with the increase in the charge of the sphere, Bjerrum length, length of LPE chain, and salt concentration. While the complex shows more wrapping degrees with decreasing of pH value. The charge inversion phenomena of dendrimer by oppositely charged LPE chain was shown to increase with increasing of above mentioned parameters, except the pH values which shows more charge reversal of dendrimer when it decreases. These results are in agreement with computer simulations (Luylin et al., 2005; Larin et al., 2010; Tian and Ma, 2010; Nandy and Maiti, 2011) and theoretical studies (Mateescu et al., 1999; Netz and Joanny, 1999; Nguyen and Shklovskii, 2001; Schiessel et al., 2001; Boroudjerdi et al., 2011).

The wrapping length of the LPE chain of length 1472.5nm around dendrimer of different generations G2, G4, G6, and G8 in the aggregate, doesn't change significantly irrespective how much dendrimer contracts due to the complexation with the oppositely charged LPE chain. As a consequence the net charge of the complexes doesn't change which is negative for all aggregates of different generations with the exception of G4. In other words the aggregate formed by dendrimer G4 – LPE complexes bears a slightly positive and fixed total charge whatever the dendrimer contracts.

The influence of the salt concentration on the complexation between LPE chain – dendrimer of different generations has been studied. we concluded that the wrapping length of the LPE chain depends on dendrimer generations. For lower generations G1 – G4, the optimal wrapping length of LPE around dendrimer increases significantly, as more and more of the LPE chain charges get neutralized. This could mean that the size of the aggregate of the complexes will increase. Whereas for higher generation G6 – G8, there is no significant increase in the optimal wrapping length of LPE chain around dendrimer, this means that the aggregate formed by the complexation between LPE and dendrimers of higher generations is insensitive to ionic strength. In other words the aggregate formed from the complexation between LPE chain with dendrimers of higher generation seems to be more neutralized than those formed of lower generations. This result is in agreement with the experimental study carried by (Carnerup et al., 2011).

The influence of the chain rigidity on the net charge of the PE – dendrimer complex has been studied. We concluded that, for a strong electrostatic interaction between LPE and dendrimer, *i.e.*, at large values of Bjerrum length. The LPE chain – dendrimer complex bears a slightly constant positive net charge irrespective how much the chain is stiff. Whereas for a weak attractive electrostatic the total charge of the complex increases considerably toward the positive sign.

In conclusion, the model presented for complexation of LPE with penetrable sphere is suitable to represent the complexation of DNA with dendrimer. As a lot of our results are in agreement with a series of computer simulations carried by Lyulin and co-workers.

Despite of this, minor modifications could be inserted on the developed model. For a strongly charged spherical complex of charge $Z(l)e$, the entropic contribution of the counterions condensation should be taken into account in the charging free energy of the complex. Also, for highly charged LPE chain, the repulsive electrostatic between the charged monomers should be added to the total free energy. The present analytical study has a great practical significance and promises to be an exciting area for further research in gene therapy. We expect that more results could be obtained by this new developed model.

Appendix A: Schiessel Model

In this appendix we will present the model developed by Schiessel and co-workers (Schiessel et al., 2001) which describe the complexation between hard sphere of radius R, charge Ze and semiflexible rod of radius a = 1nm and contour length L, where $L>>R$. They restricted their study to highly charged chain as the charge of PE chain per unit length is $-e / b$, where b the distance between the charge on the chain equals to 0.17nm which is much smaller than Bjerrum length l_B. According to the experimental conditions, the salt solution characterized by Bjerrum length $l_B = e^2/\varepsilon k_B T$ (ε: dielectric constant of the medium; at room temperature gives l_B = 0.71nm) and Debye screening length is $\kappa^{-1} = (8 c_s \pi l_B)^{-1/2}$ (c_s: Concentration of salt; κ^{-1} value is large compared to the radius of the sphere).

The total free energy for a system consists from a PE chain and a single hard sphere was proposed by them as follows:

$$F(l) = F_{compl}(l) + F_{chain}(L-l) + F_{compl-chain}(l) + F_{elastic}(l) \qquad (A.1)$$

Where L is the contour length of the DNA, and $\boldsymbol{l}$ is the length of the part of the chain wrapped around the hard sphere (Dendrimer).

The first term is the electrostatic charging free energy of a spherical complex of charge $Z(l)e$.

$$F_{compl}(l) \cong \begin{cases} \dfrac{e^2 Z^2(l)}{2\varepsilon R} & \text{for} \quad |Z(l)| < Z_{\max} \\ |Z(l)| k_B T \omega(Z(l)) & \text{for } |Z(l)| >> Z_{\max} \end{cases} \qquad (A.2)$$

Here, k_B is Boltzmann constant, Z_{max} is the effective charge of the sphere and of order $\Omega R/l_B$ (Alexander et al., 1984), $Z(l) = Z - l/b$ and ε is the dielectric constant of water.

Where $\omega(Z(l))$ is the entropic cost to confine counterions close to highly charged sphere.

$$\omega(Z(l)) = 2\ln\left(\frac{|z(l)| l_B \kappa^{-1}}{R^2}\right) \qquad (A.3)$$

The second term of the total entropic electrostatic free energy of the remaining chain ($\boldsymbol{L-l}$) has been given by

$$F_{chain}(L-l) \cong \frac{k_B T}{b} \Omega(a)(L-l) \qquad (A.4)$$

Where $\Omega(a)$ is the entropic cost to 'confine' counterions close to the chain and given by

$$\Omega(a) = 2\ln\left(\frac{4\xi\kappa^{-1}}{a}\right) \qquad (A.5)$$

And a Manning parameter, describing counterions condensation on the chain

$$\xi = \frac{l_B}{b} \qquad (A.6)$$

The third term is the electrostatic free energy of the interaction between the complex and the remainder of the chain (unwrapped part), given by

$$F_{compl-chain}(l) \cong Z(l)k_BT\ln(\kappa R) \qquad \text{(A.7)}$$

Where $Z(l)$ is the effective charge of the complex, and κ is the inverse of Debye screening length.

The final term is the elastic (bending) free energy required to bend l of the chain of Radius R around hard sphere.

$$F_{elastic}(l) \cong \frac{k_BTl_p}{R^2}l \qquad \text{(A.8)}$$

l_p is the persistence length of the chain as defined above and R the radius of the PE chain.

Schiessel extended his model for a system consisting of one PE chain and N number of hard spheres, he expressed the free energy for the aggregate by:

$$F(N,l) = NF(l) + F_{\text{int}}(N,l) \qquad \text{(A.9)}$$

Where $F(l)$ is the total free energy of the PE chain-sphere complex as expressed in Eq. (A.1), F_{int} is the electrostatic repulsion between all complexes on the beads – on – a – string configuration, and is obtained from summing over the electrostatic repulsion between all complexes within one molecule. The repulsive electrostatic interaction free energy can be expressed as

$$F_{\text{int}}(N,l) \cong \Lambda k_BT\frac{Nl_BZ^2(l)}{D(N,l)} \qquad \text{(A.10)}$$

$D(N,l)$ is the center-to-center distance between two neighboring spheres and equal $(L - Nl + 2NR) / N$, Λ is logarithmic factor of the order $\ln(\kappa^{-1}/ D)$.

Eq. (A.10) worths noting that this term will be small if the complex charge is close to neutral when $Z(l=l_{iso}) = 0$.

The total free energy for PE – dendrimer aggregate in Eq. (A.9) can be expressed as

$$\frac{F_{\text{int}}(N,l)}{k_BT} \cong \frac{l_BN}{2R}Z^2(l) + A\frac{l}{b}N - N\omega Z + \frac{\Lambda N^2l_BZ^2(l)}{D(N,l)} + \ln(\kappa R)NZ \qquad \text{(A.11)}$$

With

$$A = \frac{l_pb}{R^2} - \ln(\kappa R) - \Omega \qquad \text{(A.12)}$$

Appendix B: Electrostatic interaction between two penetrable spheres

If a uniformly charged sphere immersed in a liquid containing N ionic species with valence z_i and bulk concentration n_i (i=1, 2, …, N) The electric potential $\varphi(\boldsymbol{r})$ at position $\boldsymbol{r}$, measured relative to the bulk solution phase, given by Poisson equation (Ohshima, 2010).

$$\Delta\varphi(r) = -\frac{\rho_{el}(r)}{\varepsilon_r\varepsilon_0} = -\frac{\rho_{el}(r)}{\varepsilon} \tag{B.1}$$

Where Δ is the Laplacian, $\varepsilon = \varepsilon_r\varepsilon_0$, ε_r is the relative permittivity of the electrolyte solution, and ε_0 is the permittivity of the vacuum. The distribution of the electrolyte ions $n_i(\boldsymbol{r})$ obeys Boltzmann law, given by

$$n_i(r) = n_i^{\infty} e^{-\frac{z_i e\varphi(r)}{k_B T}} \tag{B.2}$$

Where n_i^{∞} is the concentration of the total number of ions in electrolyte solution, $n_i(\boldsymbol{r})$ is the concentration of the ith ion at position $\boldsymbol{r}$, e is the elementary electric charge, k_B is the Boltzmann constant, and T is the absolute temperature. The charge density ρ_{el} ($\boldsymbol{r}$) at position $\boldsymbol{r}$ is given by

$$\rho_{el}(r) = \sum_{i=1}^{N} z_i e n_i(r) = \sum_{i=1}^{N} z_i e n_i^{\infty} e^{-\frac{z_i e\varphi(r)}{k_B T}} \tag{B.3}$$

Substituting Eq. (B.3) into Eq. (B.1) gives:

$$\Delta\varphi(r) = -\frac{1}{\varepsilon}\sum_{i=1}^{N} z_i e n_i^{\infty} e^{-\frac{z_i e\varphi(r)}{k_B T}} \tag{B.4}$$

This is the Poisson-Boltzmann equation for the potential distribution $\varphi(\boldsymbol{r})$. If the potential is low, then the term

$$\left|\frac{z_i e\varphi}{k_B T}\right| << 1$$

By the expansion of the exponential terms in the summation in Eq. (B.3) gives:

$$\rho_{el}(r) = \sum_{i=1}^{N} z_i e n_i^{\infty}\left[1 - \left(\frac{z_i e\varphi(r)}{k_B T}\right) + \frac{1}{2!}\left(\frac{z_i e\varphi(r)}{k_B T}\right)^2 - \ldots\right] \tag{B.5}$$

The first term in the summation vanishes because of the condition of electroneutrality, *i.e*,

$$\rho_{el}(r) = \sum_{i=1}^{N} z_i e n_i^{\infty} \quad = 0 \tag{B.6}$$

By taking only the linear term in Eq. (B.5), then Eq. (B.4) becomes

$$\Delta\varphi(r) = \frac{1}{\varepsilon\ k_B T} \sum_{i=1}^{N} z_i^2 e^2 n_i^{\infty} \varphi(r) \tag{B.7}$$

Also Eq. (B.7) can be written in the linearized form

$$\Delta\varphi(r) = \begin{cases} \kappa^2 \varphi(r), \text{ outside the sphere} \\ \kappa^2 \varphi(r) - \dfrac{\rho}{\varepsilon}, \text{ inside the sphere} \end{cases} \tag{B.8}$$

With

$$\kappa = \left(\frac{1}{\varepsilon\ k_B T} \sum_{i=1}^{N} z_i^2 e^2 n_i^{\infty} \right)^{1/2} \tag{B.9}$$

Eq. (B.8) is the linearized Poisson-Boltzmann equation and κ is the Debye-Hückel parameter, also Eq. (B.8) is called the Debye-Hückel equation. The reciprocal of κ is called the Debye length.

The electrostatic free energy of ion-penetrable sphere and the electrostatic interaction free energy between two ion-penetrable spheres have been given by the linearized Poison-Boltzmann equation by Ohshima where he considered two identical interacting charged ion-penetrable spherical particles, (*i.e.*, two charged porous spheres) as shown in Figure B.1 of equal fixed charge density ρ and equal radii R, separated by a distance D between their centers (Ohshima, 1993).

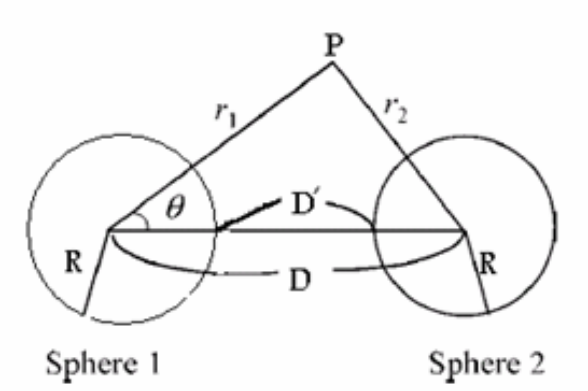

Figure B.1: Interaction between two identical charged ion-penetrable spheres of radius R, at a separation D between their centers, D' is the closest distance between their surfaces.

He considered the unperturbed potential φ_1 produced by sphere 1, since the potential of a single isolated sphere is spherically symmytric, the linearized Poison-Boltzmann equations for φ_1 depend only on r_1 and reduce to

$$\frac{d^2\varphi_1}{dr_1^2} + \frac{2}{r_1}\frac{d\varphi_1}{dr_1} = \kappa^2 \varphi_1, \ r_1 > R \tag{B.10}$$

$$\frac{d^2\varphi_1}{dr_1^2} + \frac{2}{r_1}\frac{d\varphi_1}{dr_1} = \kappa^2 \varphi_1 - \frac{\rho}{\varepsilon}, \ 0 \le r_1 < R \tag{B.11}$$

These equations can be solved by using the variables substitution

$$\varphi_1(r_1) = \frac{u_1(r_1)}{r_1} \tag{B.12}$$

The homogenous differential equation *i.e.,* Eq. (B.10) appears as the following

$$\frac{d^2u_1}{dr_1^2} = \kappa^2 u_1, \ r_1 > R \tag{B.13}$$

Thus Eq. (B.10) has the general solution of the form

$$\varphi_1(r_1) = E\frac{e^{\kappa r_1}}{r_1} + F\frac{e^{-\kappa r_1}}{r_1} \tag{B.14}$$

Also the non-homogenous differential equation in Eq. (B.11) can be expressed as

$$\frac{d^2u_1}{dr_1^2} - \kappa^2 u_1 = -\frac{\rho}{\varepsilon} r_1, \ r_1 > R \tag{B.15}$$

The general solution of Eq. (B.11) has the form

$$\varphi_1(r_1) = G\frac{e^{\kappa r_1}}{r_1} + H\frac{e^{-\kappa r_1}}{r_1} + \frac{\rho}{\varepsilon\ k^2} \tag{B.16}$$

Where *E*, *F*, *G*, and *H* are undetermined constants, the boundary conditions are

$$\varphi_1(r_1 \to \infty) = 0, \quad \varphi_1(R+\ ) = \varphi_1(R-), \text{ and } \left.\frac{d\varphi_1}{dr_1}\right|_{r1=R+} = \left.\frac{d\varphi_1}{dr_1}\right|_{r1=R-} \tag{B.17}$$

Then, Eqs. (B.10) and (B.11) are solved easily and subject to the above boundary conditions, give:

$$\varphi_{sphere\,1} = \frac{\rho}{\varepsilon\ \kappa^2} R\left[\cosh(\kappa R) - \frac{\sinh(\kappa R)}{\kappa R}\right]\frac{e^{-\kappa r_1}}{r_1}, \quad r_1 > R \tag{B.18}$$

The unperturbed potential produced by sphere 2, obtained by replacing $\boldsymbol{r}_1$ with $\boldsymbol{r}_2$, here $\boldsymbol{r}_2$ is the radial coordinate measured from the center of sphere 2 (see Figure B.1), which is related to $\boldsymbol{r}_1$ by the relation

$$r_2 = (D^2 + r_1^2 - 2Dr_1\cos\theta)^{1/2} \tag{B.19}$$

Gives

$$\varphi_{sphere\,2} = \frac{\rho}{\varepsilon\ \kappa^2} R\left[\cosh(\kappa R) - \frac{\sinh(\kappa R)}{\kappa R}\right]\frac{e^{-\kappa r_2}}{r_2}, \quad r_2 > R \tag{B.20}$$

Then Ohshima found the electrostatic interaction free energy between ion-penetrable spheres on the bases of Verwey and Overbeek method (Verwey and Overbeek, 1948). This

method is based on a charging process in which all the particle-fixed charges are increased at the same rate. The free energy for one sphere was obtained by the charging integral

$$F_{sphere} = \frac{1}{2}\int_{\nu} \rho\, \varphi_{sphere}\, d\nu \tag{B.21}$$

The integration is carried out over the volume υ, where $\rho\upsilon$ is the final charge on each sphere *i.e.*, $Q=Ze = \rho\upsilon$, which equals to $4\pi\rho /3R^3$, he got

$$F_{sphere}(Z) = \frac{3Z^2e^2}{8\pi\varepsilon(\kappa R)^2}\left[\cosh(\kappa R) - \frac{\sinh(\kappa R)}{\kappa R}\right]\frac{e^{-\kappa R}}{R} \tag{B.22}$$

The electrostatic interaction free energy can be expressed as the free energy of a system of two spheres at separation D between their centers minus that at infinite separation.

$$F_{\text{int}} = F(D) - F(\infty) \tag{B.23}$$

Where, $F(D)$ is the free energy of two spheres at separation D between their centers, $F(\infty)$ is the free energy of two sphere at infinite separation. To find the electrostatic interaction energy between two spheres, he needs only to obtain the potential distribution produced within sphere1 by sphere 2. Thus Ohshima wrote the charging integral in the form

$$F_{\text{int}} = \frac{1}{2}\int_{\nu} \rho\, \varphi_{sphere\,2}\, d\nu_1 \tag{B.24}$$

Using the spherical coordinates, the element volume of sphere 1 was given by

$$d\nu_1 = 2\pi r_1^2 \sin\theta\, d\theta dr_1 \tag{B.25}$$

Substituting Eq (B.20) into Eq. (B.24) and using Eq. (B.25). Then, the interaction free energy between two ion-penetrable spheres has been given by:

$$F_{\text{int}} = \frac{1}{2}\frac{\rho^2}{\varepsilon\ \kappa^2} R\left[\cosh(\kappa R) - \frac{\sinh(\kappa R)}{\kappa R}\right]\int_{\nu 1}\frac{e^{-\kappa r_2}}{r_2} d\nu_1 \tag{B.26}$$

The integral in the RHS of the above equation can be evaluated as follows:

$$\int_{\nu 1}\frac{e^{-\kappa r_2}}{r_2} d\nu_1 = 2\pi\int_0^R\int_0^\pi \frac{e^{-\kappa(D^2+r_1^2-2Dr_1\cos\theta)^{1/2}}}{(D^2 + r_1^2 - 2Dr_1\cos\theta)^{1/2}} \times r_1^2 \sin\theta dr_1 d\theta \tag{B.27}$$

$$= \frac{4\pi}{\kappa^2} R\left[\cosh(\kappa R) - \frac{\sinh(\kappa R)}{\kappa R}\right]\ \frac{e^{-\kappa D}}{D}$$

Then, the interaction free energy between two ion-penetrable spheres can be expressed as:

$$F_{\text{int}} = \frac{2\pi\rho^2}{\varepsilon\ \kappa^4} R^2 \left[\cosh(\kappa R) - \frac{\sinh(\kappa R)}{\kappa R} \right]^2 \frac{e^{-\kappa D}}{D} \tag{B.28}$$

References

Ainalem, M. L., Carnerup, A. M., Janiak, J., Alfredsson, V., Nylander, T., (2009), Condensing DNA with poly(amido amine) dendrimers of different generations: means of controlling aggregate morphology, Soft Matter, 5, 2310–2320.

Alexander, S., Chaikin, P. M., Grant, P., Morales, G. J., Pincus, P., Hone, D., (1984), Charge, renormalization, osmotic-pressure and bulk modulus of colloidal crystals: Theory, Chemical Physics, 80, 5776-5781.

Arcesi, L., Penna, G, L., Perico, A., (2007), Generalized Electrostatic Model of the Wrapping of DNA around Oppositely Charged Proteins, Biopolymers, 86, 127-135.

Atkinson, T., (2008), vector-mediated gene therapy, and relevance of toll-like receptors: A review of problems, progress, and possibilities, J. Cystic fibrosis, Curr. Gene Ther., 8, 201–207.

Bielinska, A. U., Chen, C., Johnson, J., Baker, J. R., (1999), DNA Complexing with Poly(amidoamine) Dendrimers, Implications for Transfection, Bioconjugate Chem., 10, 843–850.

Bjerrum, N. J., (1959), Trans. Faraday Soc., 55, x001-x003.

Bloomfield, V. A., (1997), DNA condensation by multivalent cations, Biopolymers, 44, 269–282.

Boroudjerdi, H., Naji, A., Netz., R. R., (2011), Salt Modulated Structure of Polyelectrolyte-Macroion Complex Fibers, cond. mat. soft, 1-17.

Cakara, D., Kleimann, J., Borkovec, M., (2003), Microscopic protonation equilibria of poly(amidoamine) dendrimers from macroscopic titrations, Macromolecules, 36, 4201.

Carnerup, A. M., Ainalem, M. L., Viveka, A., Nylender, T., (2011), Condensation of DNA using poly(amido amine) dendrimers: effect of salt concentration on aggregate morphology, Soft Matter, 7, 760–768.

Cheng, Y., Zhenhua, X., Minglu, M., Tongwen, X., (2008), Dendrimers as drug carriers: applications in different routes of drug administration, J. Pharm. Sci., 97, 123–143.

DeLong, R., Stephenson, K., Loftus, T., Fisher, M., Alahari, S., Nolting, A., Juliano, R. L., (1997), Characterization of complexes of oligonucleotides with polyamidoamine starburst dendrimers and effects on intracellular delivery, J. Pharm. Sci., 86, 762.

Dootz, R., Cristina T., Pfohl, T., (2011), PAMAM6 dendrimers and DNA: pH dependent "beads-on-a-string" behavior revealed by small angle X-ray scattering.

Fant, K., Esbjorner, E. K., Lincoln, P., Norden, B., (2008), DNA Condensation by PAMAM Dendrimers: Self-Assembly Characteristics and Effect on Transcription Biochemistry, 47, 1732-1740.

Fant, K., Esbjorner, E. K., Jenkins, A., Grossel, M. C., Lincoln, P., Norden, B., (2010), Effects of PEGylation and acetylation of PAMAM dendrimers on DNA Binding, cytotoxicity and in vitro transfection efficiency, Mol. Pharm., 7, 1743–1746.

Guinn, B. A., Mulherkar, R. (2008), International progress in cancer gene therapy, Cancer Gene Ther., 15, 765–775.

Hagerman P., J., (1988), Flexibility of DNA, Annual Review of Biophysics and Biophysical Chemistry, Vol. 17: 265-286.

Halford, B., (2005), Dendrimers branch out, Chem. Eng. News, 83, 30–36.

Hosam G., abdelhady, Stephanie, A., Martyn, C., Davies, C. G., Reberts, H. B., Philip M. W., (2003), Direct real‐time molecular scale visualisation of the degradation of condensed DNA complexes exposed to DNase I. Nucleic Acids Res., 31, 4001-4005.

Itaka, K., Kataoka, K., (2009), Recent development of nonviral gene delivery systems with virus-like structures and mechanisms, Eur J. Pharm Biopharm., 71, 475–483.

Jackson, J. L., Chanzy, H. D., Booy, F. P., Drake, B. J., Tomalia, D. A., Bauer, B. J., Amis, E. J., (1998), Visualization of dendrimer molecules by transmission electron (TEM): staining methods and Cryo-TEM of vitrified solutions, Macromolecules, 31, 6259–6265.

Kabanov, V. A., Sergeyev, V. G., Pyshkina, O. A., Zinchenko, A. A., Zezin, A. B., Joosten, J. G. H., Brackman, J., Yoshikawa, K., (2000), nterpolyelectrolyte Complexes Formed by DNA and Astramol Poly(propylene amine) Dendrimers, Macromolecules, 33, 9587–9593.

Kataoka K, Harashima H., (2001), Gene delivery systems: viral vs non-viral vectors. Adv Drug Deliv Rev., 52. 151.

Kukowska-Latallo, J. F., Bielinska, A., Johnson, J., Spindler, R., Tomalia, D. A., Baker, J. R., (1996), Efficient transfer of genetic material into mammalian cells using Starburst polyamidoamine dendrimers, Proc. Natl. Acad. Sci., 93, 4897.

Kukowska-Latallo, J. F., Candido, K. A., Cao, Z., Nigavekar, S. S., Majoros, I. J., Thomas, T. P., Balogh, L. P., Khan, M. K., Baker, J. R. (2005), Nanoparticle Targeting of Anticancer Drug Improves Therapeutic Response in Animal Model of Human Epithelial, J. Synthesis, 65, 5317–5324.

Kunze, K. K., Netz, R. R., (2002), Complexes of semiflexible polyelectrolytes and charged spheres as models for salt-modulated nucleosomal structures, physical review E 66, 011918, 1-28.

Kwak, J. C. T., Ed., Dekker, (1998), Polymer-Surfactant Systems New York, Vol. 77.

Larin, S. V., Lyulin, S. V., Darinskii, A. A., (2009), Charge Inversion of Dendrimers in Complexes with Linear Polyelectrolytes in the Solutions with Low pH Polymer Science, Ser ., 51, 459–468.

Larin, S.V., Darinskii, A. A., Lyulin, A. V., Lyulin, S. V., (2010), Linker Formation in an Overcharged Complex of Two Dendrimers and Linear Polyelectrolyte, J. Phys. Chem., 114, 2910-2919.

Lasic, D. D., Strey, H., Stuart, M. C. A., Podgornik, R., Federik, P. M., (1997), The Structure of DNA-Liposome Complexes, J. Am. Chem. Soc., 119, 832.

Lee, C. C., Mackay, J. A., Frechet, J. M. J., Szoka, F. C., (2005), Designing dendrimers for biological applications, Nat. Biotechnol., 23, 1517–1526.

Lee, H., Larson, R. G., (2009), Multiscale Modeling of Dendrimers and Their Interactions with Bilayers and Polyelectrolytes, Molecules, 14, 423-438.

Likos, C. N., Rosenfeldt, S., Dingenouts, N., Ballauff, M., Werner, N. Vogtle, F. (2002), Gaussian effective interaction between flexible dendrimers of fourth generation: a theoretical and experimental study, J. Chem. Phys., 117, 1869-1877.

Lindman, B., Thalberg, K., (1993), Polymer-Surfactant Interactions-Recent Developments. In Interactions of Surfactants with Polymers and Proteins, CRC Press, Boca Raton, FL, p 203.

Luo, D., Saltzman, W. M., (2000), Synthetic DNA delivery systems, Nat. Biotechnol.,18, 33–37.

Luo, D., Haverstick, K., Belcheva, N., Han, E., Saltzman, W. M., (2002), Poly(ethylene glycol)-Conjugated PAMAM Dendrimer for Biocompatible High-Efficiency DNA Delivery, Macromolecules, 35, (9), 3456-3462.

Lyulin, S. V., Darinskii, A.A., Lyulin, A. V., (2005), Computer Simulation of Complexes of Dendrimers with Linear Polyelectrolytes, Macromolecules, 38, 3990-3998.

Lyulin, S.V., Vattulainen, L., Gurtovenko, A. A., (2008), Complexes Comprised of Charged Dendrimers, Linear Polyelectrolytes, and Counterions: Insight through Coarse-Grained Molecular Dynamics Simulations. Macromolecules, 41, 4961-4968.

Maiti, P. K., Bagchi, B., (2006), Structure and dynamics of DNA-dendrimer complexation: Role of counterions, water, and base pair sequence, Nano Lett., 6, 2478-2485.

Mandelkern, M., Elias, J. G., Eden, D., Crothers, D. M., (1981), The dimensions of DNA in solution, Journal of Molecular Biology, 152, 153.

Manning Q., (1978), Counterion condensation theory, Revs. Biophys. 11, 179-24.

Martin-Herranz, A., Ahmad, A., Evans, H. M., Ewert, K., Schulze, U., Safinya, C. R., (2004), Surface functionalized cationic lipid-DNA complexes for gene delivery: PEGylated lamellar complexes exhibit distinct DNA-DNA interaction regimes, J. Biophys., 86, 1160–1168.

Mateescu, E. M., Jeppesen, C., Pincus, P., (1999), Overcharging of a spherical macroion by an oppositely charged polyelectrolyte, Europhys. Lett., 46, 493.

Nandy, B., Maiti, P. K., (2011), DNA compaction by a Dendrimer, J. Phys. Chem.,B 115, 217-230.

Netz, R. R., Joanny, J. F., (1999), Complexation between a Semiflexible Polyelectrolyte and an Oppositely Charged Sphere, Macromolecules, 32, 9026

Newkome, G. R., Yao, Z. Q., Baker, G. R., Gupta, V. K. (1985), Micelles Part 1. Cascade molecules: a new approach to micelles, J. Org. Chem., 50, 155–158.

Niu, Y. H., Sun, L., Crooks, R. A., (2003), Determination of the intrinsic proton binding constants for poly(amidoamine) dendrimers via potentiometric pH titration, Macromolecules, 36, 5725.

Nguyen, T. T., Shklovskii, B. I., (2001), Overcharging of a macroion by an oppositely charged polyelectrolyte, Physica, A 293, 324–338.

Ohshima, H., Kondo, T., (1993), Electrostatic Double-Layer Interaction between Two Charged Ion-Penetrable Spheres: An Exactly Solvable Model, Journal of Colloid and Interface Science, 499-505.

Ohshima, H., (2010), Biophysical Chemistry of Biointerfaces, John Wiley Sons, Inc., Hoboken, New Jersey.

Örberg, M. L., Schillen, K., Nylander, T., (2007), Dynamic Light Scattering and Fluorescence Study of the Interaction between Double-Stranded DNA and Poly(amido amine) Dendrimers Biomacromolecules, 8, 1557.

Park, S. Y, Bruinsma, R. F., Gelbart, W. M., (1999), Spontaneous overcharging of macro-ion complexes, Europhys. Lett., 46,454.

Prajapati, R. N., Tekade, R. K., Gupta, U., Gajbhiye, V., Jain, N. K., (2009), Dendimer-Mediated Solubilization, Formulation Development and in Vitro- in Vivo Assessment of Piroxicam, Synthesis, 6, 940–950.

Qamhieh, K., Nylander, T., Ainalem, M. L., (2009), Analytical Model Study of Dendrimer/DNA Complexes, Biomacromolecules, 10, 1720.

Qamhieh, K., Nylander T., Dias R. S., Ainalem, M. L., (in progress), Analytical Model Study of Complexes Formed between DNA and Poly(amido amine) Dendrimers of Different Generations.

Richmond, T. J., Davey, C. A. (2003), The structure of DNA in the nucleosome core, Nature, 423, 145– 150.

Rolland, A., (2005), Gene medicines: The end of the beginning? Adv Drug Deliv Rev., 57, 669–673.

Rosenfeldt, S., Dingenouts, N., Ballauff, M., Linder, P., Likos, C. N., Werner, N., Vogtle, F., (2002), Determination of the structure factor of polymeric systems in solution by small angle scattering: A SANS ‐ study of a dendrimer of fourth generation, Macromol. Chem. Phys., 203, 1995-2004.

Schiessel, H., Bruinsma, R. F., Gelbart, W. M., (2001), Electrostatic complexation of spheres and chains under elastic stress, J. of chemical physics, 115, 7245.

Schiessel, H., (2003), The physics of chromatin, J. Phys.: Condens. Matter, 15, R699-R774.

Smith, S. B., Finzi, L., Bustamante, C., (1992), Direct mechanical measurements of the elasticity of single DNA molecules by using magnetic beads, Science, 258, 1122.

Svenson, S., Tomalia, D. A., (2005), Dendrimers in biomedical applications-reflections on the field, Adv. Drug Deliv. Rev., 57, 2106–2129.

The Journal of Gene Medicine Clinical Trial site, (John Wiley and Sons, 2011), Available from: http://www.wiley.co.uk/genmed/clinical/

Tian, W., Ma, Y., (2010), Complexation of a Linear Polyelectrolyte with a Charged Dendrimer: Polyelectrolyte Stiffness Effects, Macromolecules,43, 1575-1582.

Tomalia, D. A., Baker, H., Dewald, J., Hall, M., Kallos, G., Martin, S., Roeck, J., Ryder, J., Smith, P., (1986), Dendritic macromolecules: synthesis of starburst dendrimers, j. Macromolecules, 19, 2466-2468.

Tomalia, D. A., Naylor, A. M., Goddard III, W. A., (1990), Starburst Dendrimers: Molecular-Level Control of Size, Shape, Surface Chemistry, Topology, and Flexibility from Atoms to Macroscopic Matter, Angew. Chem. Int. Ed. Engl., 29, 138–175.

Tomalia, D. A., (1993), Starburst/cascade dendrimers: fundamental building blocks for a new nanoscopic chemistry set. Aldrichim. Acta., 26, 91–101.

Tomalia, D. A., (2005), Birth of a new macromolecular architecture: dendrimers as quantized building blocks for nanoscale synthetic polymer chemistry, Prog. Polym. Sci., 30, 294–324.

Verwey, E. J. W., Overbeek , J. Th. G., (1948), Theory of the stability of Lyophobic Colloids. Elsevier, Amsterdam.

Wang, R., Zhou, L., Zhou., G., Li, G., Zhu, B., Gu, H., Jiang, X., Li., H., Wu, J., He, Guo L., , Zhu X.B., Yan, D., (2010), Synthesis and gene delivery of poly(amido amine)s with different branched architecture. Biomacromolecules, 11, 489–495.

Watson, J., Crick, F., (1953), Molecular structure of nucleic acids; a structure for deoxyribose nucleic acid. Nature, 171, 737.

Wolfert, M. A., Schacht, E. H., Toncheva, V., Ulbrich, K., Nazarova, O., and Seymour, L. W., (1996), Characterization of Vectors for Gene Therapy Formed by Self-Assembly of DNA with Synthetic Block Co-polymers. Hum. Gene Ther., 7, 2123-2133 .

Yoo, H., Sazani, P., Juliano, R. L., (1999), PAMAM Dendrimers as Delivery Agents for Antisense Oligonucleotides, Pharm. Res., 16, 1799.

Youjin, S., Jun Y., (2009), the treatment of hemophilia A: From protein replacement to AAV-mediated gene therapy, Biotechnol. Lett., 31, 321–328.

Zinchenko, A. A., Chen, N., (2006), Compaction of DNA on nanoscale three-dimensional templates, J. Phys.: Condens. Matter, 18, R453.

الملخص

لقد تمت دراسة عملية الترابط أو التجمع بين الدندريمر والحمض النووي باستخدام نموذج نظري جديد يصف التفاعل بين (LPE chain) وكرة قابلة للإختراق من قبل الأيونات المحيطة بها (ion – penetrable sphere) حيث تمثل هذه الكرة الدندريمر الذي يتكون من أجيال مختلفة منها (G1) و (G2) و (G3) و (G4) و (G6) و(G8). وقد تبين لنا أن هذا النموذج يعد نموذجاً مناسباً لوصف الترابط بين الـ (Dendrimer) و (LPE chain)، حيث توافقت بعض النتائج التي حصلنا عليها مع نتائج سلسلة من برامج المحاكاة الحديثـــــــــــــة (Molecular Dynamics MD simulations).

لقد تم دراسة الطاقة الكهروستاتيكية (Electrostatic Free Energy) لكل عنصر من هذا الترابط من قبل النموذج الجديد بهدف المقارنة مع النتائج التي تم الحصول عليها عن طريق النموذج الذي وضعه شيسل والذي يمثل الترابط بين (LPE chain) وكرة غير قابلة للإختراق (Impenetrable sphere).

لقد وجد أن درجة التفاف الـ (LPE chain) حول الدندريمر تزداد بزيادة كل من شحنة الدندريمر، وتركيز الأملاح في المحلول، و طول الـ (LPE chain)، وتقل هذه الدرجة بزيادة صلابة الـ (LPE chain). أما بالنسبة للترابط او التجمع الذي يحوي العديد من الدندريمرات مع الـ (LPE chain) وهوما اطلقنا عليه مصطلح الـ (Aggregate)، تبين أن هذه الـ (Aggregate) بشكل عام تمتلك شحنة كلية ثابتة نسبياً بغض النظر عن التغير الحادث في حجم الدندريمر أثناء تفاعله مع الـ (LPE chain) ، أما بالنسبة لدرجة التفاف الـ (LPE chain) حول هذه الدندريمرات فوجد أنها تتأثر بتركيز الأملاح وخاصة لـ (Aggregate) التي تتكون من أجيال صغيرة مثل، (G2) و (G4) فهي تزداد بشكل واضح مع زيادة تركيز الأملاح اما التي تتكون من أجيال كبيرة مثل، (G6) و (G8) فقد أظهرت النتائج أن درجة التفاف (LPE chain) حول الدندريمرات كانت شبه معدومة.